

**TESTING AND NUMERICAL MODELING OF  
MECHANICALLY STABILIZED EARTH WALL  
REINFORCED WITH GEOTEXTILE**

**A THESIS**

*Submitted in partial fulfillment of the requirements for the award of the degree  
of*

**BACHELOR OF TECHNOLOGY**

**IN**

**CIVIL ENGINEERING**

Under the supervision of

**Dr. Saurabh Rawat  
(Assistant Professor)**

*By*

*Manik Uppal (141690)  
Hannaan Malik (141692)*

**to**



**JAYPEE UNIVERSITY OF INFORMATION TECHNOLOGY**

**WAKNAGHAT, SOLAN – 173234**

**HIMACHAL PRADESH, INDIA**

**May-2018**

## Certificate

This is to certify that the work which is being presented in the project report titled “**TESTING AND NUMERICAL MODELING OF MECHANICALLY STABILIZED EARTH WALL REINFORCED WITH GEOTEXTILE**” in partial fulfillment of the requirements for the award of the degree of Bachelor of Technology in Civil Engineering and submitted to the Department of Civil Engineering, Jaypee University of Information Technology, Waknaghat is an authentic record of work carried out by **Manik Uppal (141690), Hannaan Malik (141692)** during a period from January 2018 to May 2018 under the supervision of **Dr. Saurabh Rawat**, Assistant Professor, and co –supervision of **Dr. Ashok Kumar Gupta**, Professor and Head, Department of Civil Engineering, Jaypee University of Information Technology, Waknaghat.

The above statement made is correct to the best of our knowledge.

Date: .....

Dr. Ashok Kumar Gupta  
Professor & Head of  
Department  
Department of Civil  
Engineering  
JUIT Waknaghat

Dr. Saurabh Rawat  
(Supervisor)  
Assistant Professor  
Department of Civil  
Engineering  
JUIT Waknaghat

External Examiner

## **ACKNOWLEDGEMENT**

Every project from micro to macro level undergoes a journey and is made successful largely due to the effort of a number of wonderful people who give in their valuable time and advice or lent a helping hand. I sincerely appreciate the inspiration; support and guidance of all those people who have been instrumental in making this project a success.

First of all, I would like to acknowledge the people who mean a lot to me, my parents, for showing faith in me and giving me liberty to choose what I desire. I salute them for the selfless love, care, pain and sacrifice they did to shape my life.

It is my radiant sentiment to place on records my best regards, and a deepest sense of gratitude to Dr. Ashok Kumar Gupta, Head of the Department Civil Engineering, Jaypee University of Information Technology for his precious guidance which was extremely valuable asset for my study, theoretically and practically.

A word of thanks to the project supervisor Dr. Saurabh Rawat who dedicated his time and effort to help the team achieve the desired results. It was his encouragement and guidance that helped the team to progress. I would like to appreciate the guidance and help provided by the lab assistants in performing the various tests and obtaining the results.

I would like to appreciate the guidance provided by other supervisors and the panel members, especially regarding our project presentations, which helped us to improve and enhance our presentation and communication skills.

## Abstract

This study briefly describes the scope of improvisation in classical soil reinforcement techniques. Such techniques have come a long way from gravity retaining walls, to reinforced concrete types, to buttresses and counterfort walls, to mechanically stabilized earth wall. In the present study physical tests have been carried out on reinforced soil retaining wall subjected to uniform loading. Model of retaining walls are constructed in a perspex box reinforced with multifilament polypropylene geotextile reinforcement using the wrap around technique with dry sand as the backfill soil. The desired unit weight of the backfill was achieved using pluvation technique (rainfall technique). Instrumentation included the use of dial gauges to measure the corresponding displacement.

The second part of the present study involves validation of the model testing by numerical modeling using FEM (finite element method). For the desired purpose PLAXIS 2D software was used. Horizontal and vertical displacements have been recorded, analyzed and compared with the results obtained from model testing. The validation of model testing results with numerical modeling using finite element method reveals that a horizontal displacement of 13mm is obtained under a load bearing capacity of  $130 \text{ kg/cm}^2$ , whereas under a load of  $110 \text{ kg/cm}^2$  is found to give a horizontal displacement of 13mm from finite element analysis.

**Keywords:** mechanically stabilized earth wall; geotextile; horizontal displacement; load bearing capacity; finite element method; Plaxis 2D

# TABLE OF CONTENTS

	<b>PAGE NO.</b>
Certificate	ii
Acknowledgement	Iii
Abstract	iv
Table of Contents	v
List of Tables	vii
List of Figures	viii
List of Acronyms	x
<b>1. INTRODUCTION</b>	
1.1 General	1
1.2 Mechanically Stabilized Earth Walls	2
1.3 Mechanically Stabilized Earth Theory	
1.4 Applications of MSE wall	2
1.5 Reinforcement	4
1.6 Geotextile	5
1.7 Reinforcement Spacing	6
1.8 Backfill Soil	7
1.9 Advantages and Limitations	7
1.9.1 Advantages	7
1.9.2 Limitations	8
1.10 Organization of Thesis	8
<b>2. LITERATURE REVIEW</b>	
2.1 General	10
2.2 Research work on MSE wall	10
2.3 Summary of Literature Review	20
2.4 Objectives	21
<b>3. METHODOLOGY</b>	
3.1 General	22
3.2 Material Used	22
3.2.1 Woven Polypropylene Geotextile	22
3.2.2 Model Tank	23
3.3 Soil Tests	24
3.3.1 Sieve Analysis	24
3.3.2 Direct Shear Test	25
3.4 MSE Wall Preparation	28
3.5 Instrumentation	29
3.5.1 Foil Strain Gauges	29

3.5.2 Digital Multimeter	30
3.5.3 Wheatstone Bridge	31
3.5.4 Connecting Wires	31
3.6 Model Testing	34
<b>4. NUMERICAL MODELING</b>	
4.1 General	36
4.2 Material Properties	37
4.3 Model Configuration	38
4.4 Mesh Generation	39
4.5 Initial Stress Distribution and Loading	40
<b>5. RESULTS AND DISCUSSIONS</b>	
5.1 General	42
5.2 Laboratory Results and Discussions	42
5.2.1 Sieve Analysis	42
5.2.2 Direct Shear Test	44
5.3 Load-Displacement under Footing	46
5.4 Results from Numerical Modeling	48
5.4.1 Displacements	48
5.4.2 Stresses	50
5.4.3 Failure of MSE Wall	50
5.5 Validation of Experimental Testing by Numerical Modeling	51
<b>6. CONCLUSION</b>	
6.1 General	56
6.2 Conclusions	56
6.3 Scope of Future Work	57

## **REFERENCES**

**ANNEXURE A**

**ANNEXURE B**

**ANNEXURE C**

## **LIST OF TABLES**

<b>TABLE NO.</b>	<b>DESCRIPTION</b>	<b>PAGE NO.</b>
2.1	Typical Minimum Length of Reinforcement	12
2.2	Factor of Safety against various failure mechanisms	15
3.1	Specifications of Woven Polypropylene Geotextile	23
3.2	Size of sieves used	27
3.3	Resistance of arms of four wheatstone bridge	35
3.4	Input Voltages	35
4.1	Material Properties used in Numerical Simulation	38
5.1	Particle Size Distribution Table	44
5.2	Values of Normal Stress and Shear Stress	45
5.3	Values of Normal Stress and Shear Stress	46

## LIST OF FIGURES

FIGURE NO.	DESCRIPTION	PAGE NO.
Fig 1.1	Generic cross-section of an MSE structure	1
Fig 1.2	Free-Body diagram of load transfer in an MSE wall	2
Fig 1.3	MSE wall applications	4
Fig 1.4 (a)	Woven Geotextile	5
Fig 1.4 (b)	Non-Woven Geotextile	5
Fig 1.4(c)	Knitted Geotextile	6
Fig 2.1	Emperical curve to estimate lateral displacement during construction of MSE wall	12
Fig 2.2	Modes of Failure	14
Fig 2.3(a)	Inclinometer reading results and comparison with predicted values	16
Fig 2.3(b)	Result of geodetic survey of wall face and comparison with predicted values	16
Fig 2.4	Effect of reinforcement length on horizontal displacement of MSE wall	17
Fig 2.5	Comparison of reinforced earth wall with different types of reinforcing elements	19
Fig 3.1	Woven Polypropylene Geotextile	22
Fig 3.2 (a)	Model Tank (Top View)	24
Fig 3. 2(b)	Model Tank (Side View)	24
Fig 3.3	Scheme of DST performed	27
Fig 3.4	Shear Box with Geotextile	27
Fig 3.5	Various stages of MSE wall fabrication	29
Fig 3.6	Strain Gauge	30
Fig 3.7	Digital Multimeter	30
Fig 3.8	Wheatstone Bridge Circuit	31
Fig 3.9	Connecting Wires	31
Fig 3.10(a)	Setup of wheatstone bridge circuit	32
Fig 3.10(b)	Project Board	33
Fig 3.10(c)	Digital multimeters to measure $V_{out}$	33
Fig 3.11	Schematic Diagram for completed setup of MSE wall	35
Fig 3.12	Fabricated Model	35

Fig 4.1	Geometry model with all structural elements	38
Fig 4.2	Generated Mesh at Initial Conditions	39
Fig 4.3	Effective Stress Distribution	40
Fig 4.4	Deformed Mesh under overburden pressure	41
Fig 4.5	Application of uniform distributed load	41
Fig 5.1	Particle Size Distribution Curve	43
Fig 5.2	Variation of shear stress and normal stress	44
Fig 5.3	Variation of shear stress and normal stress	45
Fig 5.4	Variation of horizontal displacement vs. pressure	46
Fig 5.5	Vertical displacement of MSE under footing	47
Fig 5.6	Variation of strain vs. pressure	47
Fig 5.7	Displacement of geotextile	49
Fig 5.8	Displacement Contours	49
Fig 5.9	Mean stresses	50
Fig 5.10	Plastic Points	51
Fig 5.11(a)	Deformed wall from Numerical Modeling	52
Fig 5.11(b)	Deformed wall from Model Testing	52
Fig 5.12(a)	Horizontal Displacement from Numerical Modeling	53
Fig 5.12(b)	Horizontal Displacement from Model Testing	53
Fig 5.13(a)	Vertical Displacement from Numerical Modeling	55
Fig 5.13(b)	Vertical Displacement from Model Testing	55

## LIST OF ACRONYMS

$\phi$	Friction Angle
$\psi$	Dilation Angle
$\nu$	Poisson's Ratio
$\gamma_{unsat}$	Unsaturated Unit Weight
$\gamma_{sat}$	Saturated Unit Weight
$c$	Cohesion
$E$	Modulus of Elasticity
$N_p$	Tensile Yield Strength
$R_{inter}$	Interface Strength

# CHAPTER 1

## INTRODUCTION

---

### 1.1 General

Mechanically stabilized earth or MSE refers to the concept of reinforcing a soil mass with artificial reinforcement. The technique of reinforcing soil mass thrives on parameters such as the type of reinforcement, reinforcement spacing and backfill soil. Throughout the history of mankind, these basic principles governing a MSE structure have been developed and refined. The various applications geosynthetics find in the field of civil engineering are discussed in this chapter along with their advantages and limitations.

### 1.2 Mechanically Stabilized Earth Walls

MSE walls find their major application in stabilization of unstable slopes and retaining the soil mass. The wall face is often made of precast or segmental blocks, panels or geocells which have the capacity to tolerate differential movement. The walls are made up of granular soil, with or without reinforcement, while the backfill soil is retained. Reinforced walls capitalize on the stabilization provided by horizontal layers, which are typically made of geogrids or geotextiles. The reinforced soil mass, in conjunction with the facing, forms the wall. Soils lack tensile strength, but MSE walls provide a popular alternative to gravity retaining walls because of the additional resistance to lateral earth pressures provided by the reinforcements. The generic cross section of an MSE structure is presented in Figure 1.1

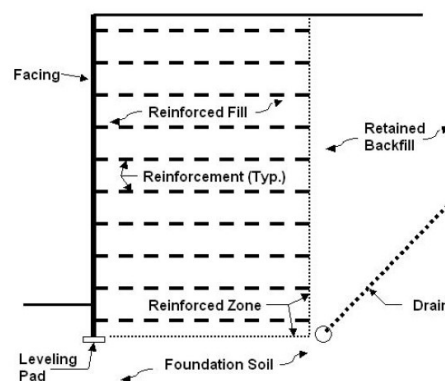


Figure 1.1 Generic cross-section of an MSE structure

### 1.3 Mechanically Stabilized Earth Theory

The connections with the facing enable the transfer of internal earth pressure from the reinforced soil mass to the soil reinforcement. The tension is then transferred to the reinforced soil beyond the active soil wedge through frictional resistance and bearing against ribs or transverse members if present. Thus, the face of the wall, soil reinforcement and the reinforced soil act as a flexible block. The free body diagram depicting the load transfer mechanism in a MSE wall is shown in Figure 1.2

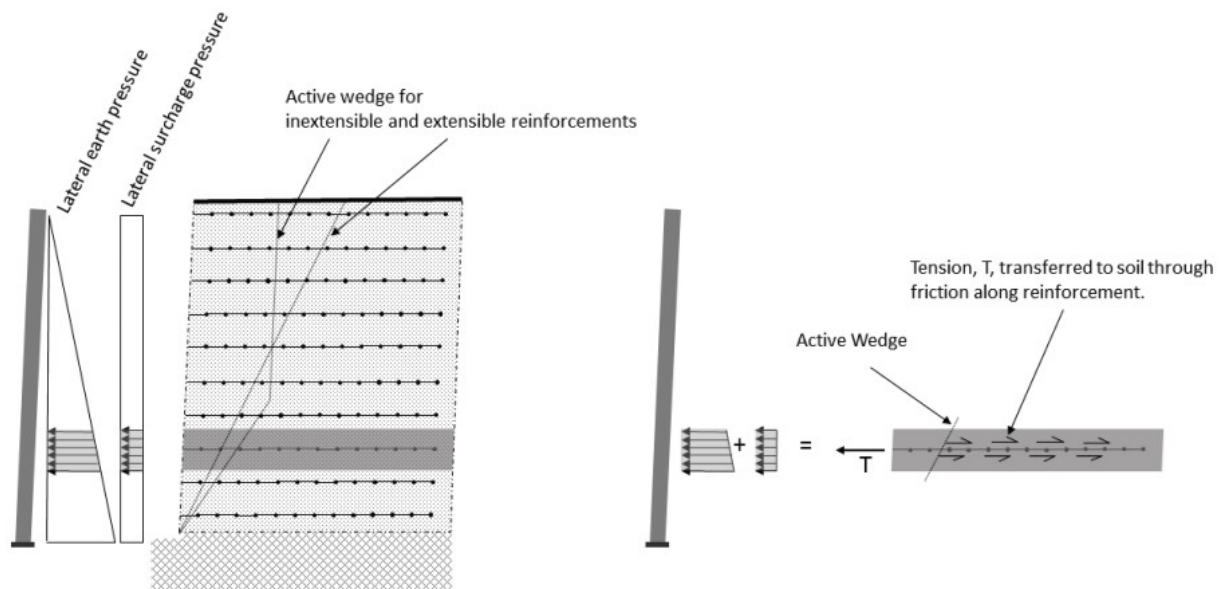


Figure 1.2 Free-body diagram of load transfer in an MSE wall

### 1.4 Applications of MSE Walls

Being a cost-effective alternative, MSEW structures tend to replace and find a place for themselves in domains where traditionally reinforced concrete or gravity walls were used to retain the soil mass. The spheres of economic constructions where MSEW structures are particularly suited include steep-sided terrain, groundwork subjected to slope instability, or in areas of poor foundation soils. In addition to technical superiority offered by MSE walls, it also eliminates the costs required for foundation improvements which may be required to support conventional structures. The various applications of a MSEW structure have been explained below.

- **Bridges** – MSEW technology is used in the design of abutments of bridge superstructures. It consists of two parts, the direct support (where abutment rests on a spread footing atop of an MSE structure) and indirect support (abutment on piles with the MSE structure supporting the fill). Such abutments can be constructed to withstand loads ranging from light (imposed by a single span bridge) to a heavily loaded one (imposed by rail and industrial structures).
- **Railway Structures** - MSEW can be used for the construction of light railways, freight carriage and high speed railway projects as they provide an increased load-carrying capacity and resistance to vibrations. Such a railway structure is very space saving and makes it possible to build walls parallel to a railway line. MSEW is to be built entirely from the backfill side and hence eliminates the need for any scaffolding or any structure in front of the wall.
- **Waterways and Dams** – MSEW are used as structures in marine environments and fresh waters. Retaining walls to support riverbanks, coastal highways, and bridge abutments along earth dams, spillways, sea walls and dock walls are few examples of construction in such an environment. Design of such structures also accounts the forces exerted by tides, flooding, debris flow, storms and sudden water drawdown.
- **Protective Structures** – Capabilities to withstand vibrations, impact, explosions, flooding and extreme temperatures make MSE structures an ideal choice for civil and military applications. These structures are so developed to store oil and natural gas vessels and provide protection against impact of explosions and spillages.
- **Commercial and Public Facilities** – MSE structures find their way into residential and public facilities as a part of support for parking garages, relief walls and access and safety ramps. Such structures have been utilized at airports, hospitals, apartments and commercial facilities. The various applications have been summarized in the diagram below.

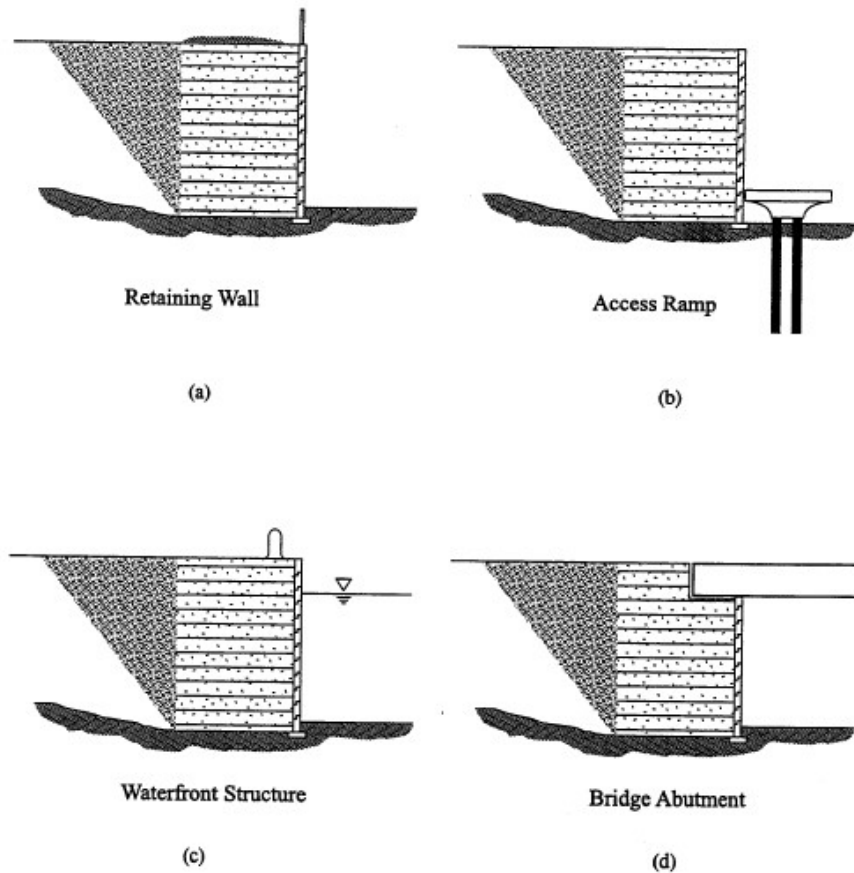


Figure 1.3 MSE wall applications (a) retaining wall; (b) access ramp; (c) waterfront structure; and (d) bridge abutment [4]

## 1.5 Reinforcement

Horizontally placed reinforcements in a MSEW provide the required tensile strength to hold the soil mass as a unit. The reinforcement materials of MSEW have varied over time. Originally, steel strips 50 -120 mm long and 2-5 inches wide were used. The strips used can be ribbed in order to provide additional friction. There also exists an option to use prefabricated pile sleeve to reduce negative skin friction on piles embedded behind MSE bridge abutments. In certain conditions, steel grids or meshes are also form a part of reinforcement. Several types of geosynthetics are used, which include geogrids and geotextiles. The main constituent of reinforcing geosynthetics are high-density polyethylene, polyester,

and polypropylene. These materials may be ribbed and are made available in various configurations. The principal requirements for a reinforcing material are as follows.

- High strength and high stability with a low tendency to undergo creep
- Durability and ease to handle
- High coefficient of friction and adherence with the soil
- Economically viable and readily available

Geosynthetics as a superset include eight main products under it – geotextiles, geogrids, geomembranes, geonets, geofoam, geosynthetic clay liners, geocomposites and geocells. Our consideration encompasses around studying the behavior and interaction of geotextiles in a MSE structure.

## 1.6 Geotextiles

Geotextiles are permeable synthetic material, which are used in combination with the soil mass. They're typically made from polymers such as polypropylene or polyester. They're typically available in three forms – woven fabrics, non woven fabrics, knitted fabrics.

- **Woven Geotextiles** – Woven geotextiles are prepared using the technique of weaving. Its appearance can be divided into two characteristic yarns, the yarn running parallel to the length is called warp and the one perpendicular is called weft. Individual threads (monofilaments, fibrillated yarns, slit films) are woven together to form a large, uniform piece. This method provides a high load capacity to the geotextile and makes them a suitable fit for road construction.

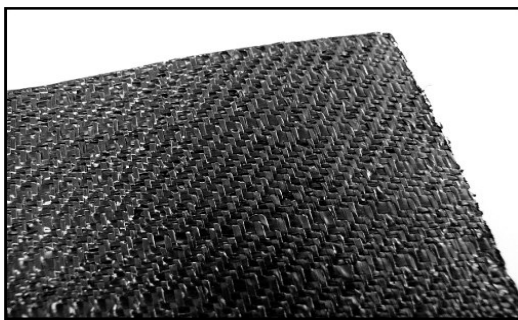


Figure 1.4 (a) Woven Geotextile



Figure 1.4 (b) Non-Woven Geotextile

- **Non-Woven Geotextiles** – Non-woven geotextiles are manufactured using short staple fibre or continuous filament yarn. Rather than weaving, these geotextiles are manufactured/ bonded together using thermal, chemical or mechanical techniques. Thermally bonded non-wovens contain wide range of opening sizes and a typical thickness of about 0.5-1 mm while chemically bonded non-wovens are comparatively thick usually in the order of 3 mm. On the other hand mechanically bonded non-wovens have a typical thickness in the range of 2-5 mm and also tend to be comparatively heavy because a large quantity of polymer filament is required to provide sufficient number of entangled filament cross wires for adequate bonding. Non-woven geotextiles are typically not suitable for stabilization or reinforcement projects.
- **Knitted Fabrics** – As the name implies, the adopted method for knitted geotextiles is knitting. A series of loops of yarn are interlocked together to produce the geotextile.

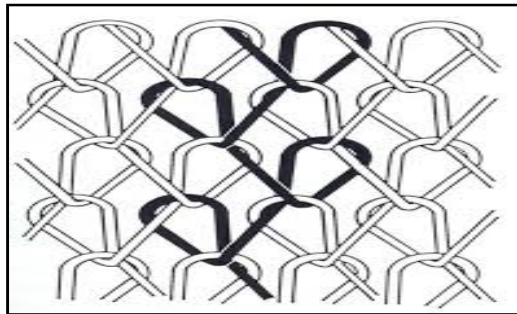


Figure 1.4 (c) Knitted Geotextile

## 1.7 Reinforcement Spacing

Reinforcement spacing is defined as the vertical distance between the horizontal layers of reinforcement. There exists an inverse relationship between the load bearing capacity of the soil and the reinforcement spacing. An increase in load bearing capacity is observed with increase in number of layers of reinforcement spaced closer together (Elias et al, 2001). However, to minimize on material and labor costs, MSE walls are designed to maximize reinforcement spacing.

## **1.8 Backfill Soil**

Since the backfill is the primary source of stresses that the MSE wall must resist, its selection becomes crucial for the design of the wall. Theoretically, any soil may be used as a backfill to increase the overall strength of the soil-reinforced composite unit. However, as a matter of choice, granular soils are the preferred backfill of MSE walls. Granular soils are well drained and help in elimination of consideration of pore water pressure.

## **1.9 Advantages and Limitations**

### **1.9.1 Advantages**

MSE walls have many advantages when compared to the conventional soil retaining structures which include reinforced concrete and concrete gravity retaining walls.

- MSE walls utilize a simple and rapid construction methodology.
- MSE walls do not require a large construction equipment setup.
- MSE walls eliminate the requirement of special skills for the construction.
- MSE walls require less site preparation and less space in front of the structure for construction operations. .
- MSE walls help in reducing the right-of-way acquisition.
- MSE walls being tolerant to deformations do not need a rigid and unyielding foundation support.
- Observations in seismically active zones have concluded that these structures demonstrate a higher resistance.
- MSE walls are cost effective when compared to other alternatives. Pre-manufactured materials and rapid construction methodology result in the cost reduction.
- MSE walls can be feasibly constructed to heights in excess of 100 ft (30 m).
- The precast concrete facing elements can be made in various shapes and textures for aesthetic considerations. Masonry units, timber and gabions can be used for this purpose.

## **1.9.2 Limitations**

MSE walls also have a set of limitations. They are as following.

- MSE walls require a large space behind the wall for the purpose of installation of the required reinforcement.
- MSE walls require a specific granular fill for its construction. At some sites, the importing cost of the required suitable fill material may make the system uneconomical.
- There exists a shared design responsibility between material suppliers and owners.

## **1.10 Organization of Thesis**

The first chapter of this thesis gives a brief insight into the concept of soil reinforcement techniques. Various applications of a mechanically stabilized earth have been discussed. The two major components required for soil reinforcement, that is, the reinforcement and the backfill soil have been discussed in detail. The chapter summarizes the advantages and limitations associated with the MSE structure.

The second chapter is a summarization of the various parametric studies and numerical analysis conducted on the concept of soil reinforcement. The chapter highlights the affect on the behavior of the reinforced structure by varying the very many parameters, namely the length of reinforcement to height of wall ratio, the stiffness of the reinforcement, the slope of the wall and the backfill soil.

The third chapter talks about the methodology adopted for the construction of the MSE wall. Before the actual construction procedure, the materials required for the construction, namely, perspex sheet, woven polypropylene geotextile, strain gauges and digital multimeters are discussed in length. The next part of the chapter deals with the tests conducted to determine the strength parameters of the soil. The last part of the chapter involves the construction procedure and the instrumentation to record the various readings.

The fourth chapter deals with the numerical modeling of the MSE wall, done to validate and account for the variations observed with respect to the experimental analysis. The software used for modeling and analyzing the model was Plaxis 2D which operates on the finite element method. The chapter deals with sequential steps performed to fabricate and analyze the model. The chapter includes the various screenshots representing the various conditions of the fabrication and loading.

The fifth chapter deals with all the results obtained. The results obtained from the laboratory tests, experimental analysis and numerical modeling have all been recorded, and tabulated and corresponding graphs have been plotted. The chapter involves the comparison and validation of the results obtained from both the mentioned analysis.

The sixth chapter is about the conclusion of the entire study conducted in this thesis. The chapter also provides an insight into the scope for future work.

The seventh chapter is a list of all the research work, studies, publications, books and websites to which we referred for the incumbent study.

## CHAPTER 2

# LITERATURE REVIEW

---

### 2.1 General

Engineers and scientists engaged in the research field have been working on designing the reinforced soil structures for the past many years. From the use of sticks and branches for reinforcing mud dwellings to pioneering the soil reinforcement by French architect and engineer Hendri Vidal, the concept of soil reinforcement has come a long way. Researches on MSE wall have included studies which have varied parameters such as the length of reinforcement to height of the wall (L/H) ratio, reinforcement stiffness, backfill, and working with various reinforcements which include synthetic as well as natural fibers. This chapter tries to summarize the various parametric studies as well as numerical analysis conducted on the concept of soil reinforcement.

### 2.2 Research work on Mechanically Stabilized Earth (MSE) wall

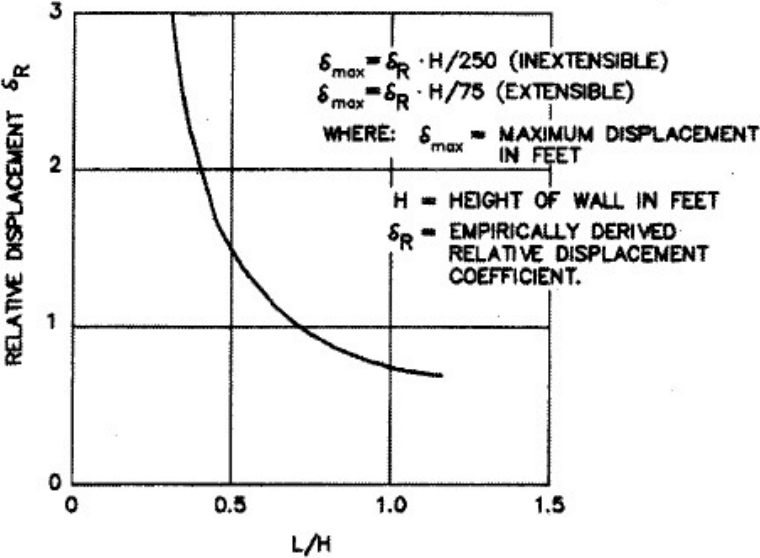
**San et al. (1994)** exhibited the correlations between the potential failure envelop and the maximum tensile force developed in the geosynthetic reinforcement using two methods, namely, Finite Element (FE) and Limit Element (LE) method respectively. The LE analysis was performed using “STRATASLOPE.” For the analysis three different reinforced slopes were prepared (75, 60 and 45 degree). Utilizing the same parameters, FE analysis was also performed. For the purpose of FE analysis, the model used was Duncan and Chang model. Coefficient of earth pressure was chosen as  $K_0$  and the critical length value of the reinforcement obtained in the LE analysis for a safety factor one, were used as initial inputs for the FE analysis. The maximum reinforcement tensile force and the failure pattern of the reinforced slopes obtained from both the methods were compared. The results obtained were identical, in terms of strength of the reinforcement and the critical slip surfaces. So, it can be concluded that utilizing a consistent value of  $K_0$  brings about an agreement between results obtained in LE and FE analysis respectively.

**Scarborough (2004)** in the work “A Tale of Two Walls: Case Histories of Failed MSE Walls” brought about the case histories of two mechanically stabilized earth (MSE) retaining walls. Both the walls were reinforced with geosynthetics and used clayey soil as the backfill. Only one wall failed while the other undergoing a large deformation, still remained in service. The author attributes the catastrophic failure of the wall to poor drainage. Lack of adequate drainage facility allowed pore water pressure to develop and this resulted into the failure of the wall. Other factors which contributed to this failure can be cited as inconsistent compaction and use of clayey soil. Due to errors in performing the global stability analysis for the wall “B”, it underwent serviceability failure which can be attributed to the inadequate geogrid reinforcements. Another contributing factor can be cited as use of clayey soil. The author provides suggestions in order to prevent such kind of failures by lowering down errors in designing and global stability analysis. All these suggestions coupled with proper drainage control will help to prevent such catastrophic failures.

Design and Construction of Mechanically Stabilized Earth Walls and Reinforced Soil Slopes – Volume I” presented by the **U.S. Department of Transportation and Federal Highway Administration (2009)** is a report that sheds light on the performance criteria of the MSE structures. The author states, that with respect to the lateral displacements, there exists no such definite method to predict them. The author argues that the horizontal movement is a result of various parameters including the compaction, reinforcement extensibility, reinforcement length, reinforcement to panel connection details, and details of the facing system. However the study presents a rough estimate of the lateral displacements based on the length of reinforcement to wall- height ratio and extensibility of reinforcement as depicted in Figure 2.1.

Figure 2.1 indicates that by increasing the L/H ratio of reinforcements from 0.5 to 0.7, the deformation can be lowered by 50 percent. The performance of the MSE structure depends on two criteria, site and structure. Structure – dependent criteria involves the safety factors determined considering the load, resistance factors and the tolerable movement of the structure. There exist a number of site specific criteria that need to be established at the initial construction phase. These include design limits and wall height, alignment limits, length of

reinforcement, external loads and wall embedment. The typical minimum reinforcement length criteria under different loadings is presented in Table 2.1



For  $L = 0.7 H$   
 Metallic (inextensible) reinforcement = ¼-in. per 10 ft of wall height  
 Geogrid (moderately extensible) reinforcement = 1 in. per 10 ft of wall height  
 Geotextile (extensible) reinforcement = 1.5 in. per 10 ft of wall height

Based on 20 ft high walls, relative displacement increases approximately 25% for every 400 psf surcharge. Experience indicates that for higher walls, the surcharge effect may be greater.

NOTE: This figure is only a guide. Actual displacement will depend, in addition to the parameters addressed in the figure, on soil characteristics, compaction effort, and contractor

Figure 2.1 Empirical curve to estimate lateral displacement during construction of MSE wall [4]

Table 2.1 Typical Minimum Length of Reinforcement [4]

Condition	Typical Minimum L/H Ratio
Static loading with or without traffic surcharge	0.7
Sloping backfill surcharge	0.8
Seismic loading	0.8 to 1.1

A study by **Hardianto et al. (2010)** reveals that more than 30,000 reinforced earth structures have been built worldwide and many of these structures have not been designed considering seismicity, yet many have performed satisfactorily. The seismic design has been previously ignored probably because static design was considered conservative and adequate for most seismic conditions. But due to the occurrence of large earthquakes between 1994 and 1999, there arose a need to consider seismicity for the purpose of MSE wall design. The most popular seismic design method for a steel reinforced MSE wall is the one based on Mononabe-Okabe pseudo static analysis, which has undergone various modifications leading to its new found place in AASHTO Bridge Design Specifications. The author anticipates that there exists a critical B/H ratio that can be developed to study the flexibility of MSE walls with increasing heights. Available information shows that MSE walls, taller than 5m tend to amplify ground acceleration more, in turn, making them more vulnerable to seismic activities than shorter walls.

A study by **Agrawal (2011)** gives an overview of the available various natural and synthetic textile fibers that are used as reinforcement. The study elaborates about the various important characteristics of Geotextiles, namely, physical, mechanical, hydraulic, degradation and endurance properties. The study broadly classifies between the natural and synthetic fibers and gives an insight into their respective synthesis procedure. The commonly used natural fibers were identified as – ramie and jute. On the other hand, synthetic fibers included polyamides, polyesters, polyethylene, polypropylene, polyvinyl chloride, ethylene copolymer bitumen and chlorinated polyethylene. The study talks about the various functions performed by the Geotextiles, namely, separation, filtration, drainage, reinforcement and sealing. Civil engineering fields where Geotextiles find their application include– road works, railway works, river canals and coastal works, sports field construction and agriculture. The author, examines that the role of nanotechnology will help in enhancement of geotextile performance. He argues that by reducing the diameter to nanoscale, an increase in surface area to the tune of  $1000\text{m}^2/\text{g}$  can be achieved.

**Krishna and Latha (2012)**, which we regard as the mother paper for the incumbent study has been used extensively. The model tank and fabricated wall dimensions were ascertained from the study conducted by the authors. The backfill material used for their study was locally available and the maximum and minimum dry unit weights were reported as 17.6

and  $14.0 \text{ kN/m}^3$ . The method adopted by the authors to achieve uniform density was the rainfall technique, also known as pluviation technique. The authors for the purpose of reinforcing the soil mass used the multifilament woven polypropylene geotextile having a mass per unit area value of  $230 \text{ g/m}^2$ . The dynamic analysis of the reinforced structure was conducted by the authors and was validated by modeling the structure numerically on FLAC. For the purpose of modeling the geotextile layers in FLAC, beam elements were utilized which gave three-degrees of freedom, namely, x and y translation and rotation. This was done to make the beam behave as a linearly elastic material and hence imitating the nature of the geotextile reinforcement. Sensitivity analysis was performed to study the affect of varying parameters on the dynamic behavior of the wall. The study concluded that amongst all the parameters, dilation and friction angle of the soil mass and the stiffness of the reinforcing geotextile are the most affecting parameters. The author recommends the backfill to be dense, in order to ensure better soil-reinforcement interaction and a more stabilized structure.

**Babu (2013)** in his lecture on “Reinforced Soil Retaining Walls – Design and Construction” mention two forms of stability that must be investigated. They include the external and internal stability. The external stability briefly consists of external sliding, overturning failure, bearing capacity and slip failure. Under the umbrella of internal stability, there exist two main failure mechanisms that need to be investigated, namely, tension failure and pull-out failure respectively. The different modes of failure are summarized in Figure 2.2

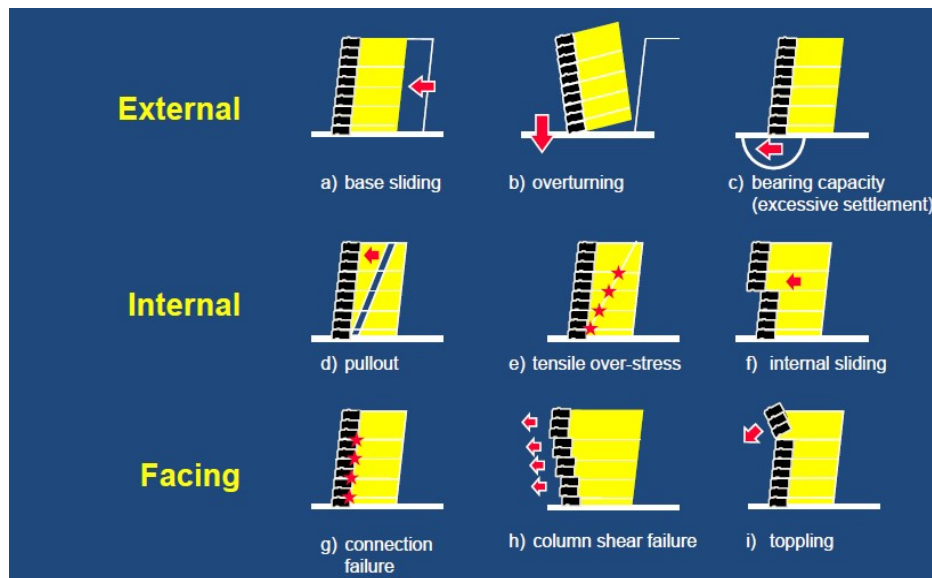


Figure 2.2 Modes of Failure [8]

Table 2.2 lists the various factors of safety against the failure mechanisms.

Table 2.2 Factors of safety against various failure mechanisms [8]

Failure Mechanism	Factor of Safety
Base Sliding	1.5
Overturning	2.0
Bearing capacity	2.0
Tensile over-stress	1.0
Pullout	1.5
Internal Sliding	1.5
Connection Failure	1.5
Column Shear Failure	1.5
Toppling	2.0
Global Stability	1.3 – 1.5

**Skejic et al. (2013)**, conducted numerical analysis of a test wall using the Plaxis Geotechnical Software Package. In the study, a plane strain numerical model was simulated. The reinforced wall was built on a stiff soil foundation. The various inputs were fed into the software and the surcharge was modeled according to the actual construction sequence by imposing a soil layer above the soil. A comparison was done between the numerically obtained and field measured displacements and is represented in Figure 2.3(a) and 2.4(b)

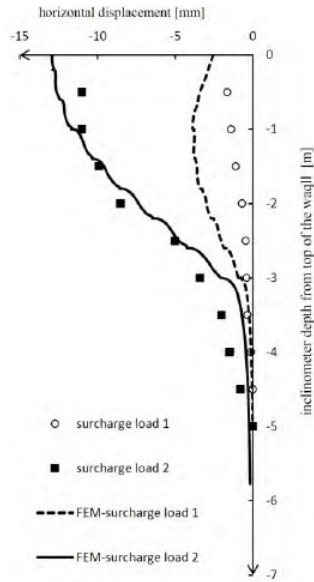


Figure 2.3(a) Inclinometer reading results and comparison with predicted values [9]

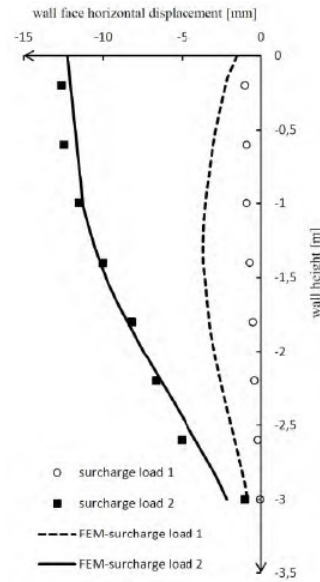


Fig 2.3(b) Result of geodetic survey of wall face and comparison with predicted values [9]

The author argues that the mismatch observed between the predicted and measured horizontal displacements in the first phase of surcharge load application is due to the inadequate soil constitutive model. On the other hand, the graphs indicate that the displacement field for the final phase of surcharge load application (larger deformations) is quite well predicted.

According to a study conducted by **Kibria et al. (2014)**, the reinforcement stiffness and L/H ratio were identified as two important parameters affecting the horizontal displacement of a MSE wall at a certain height. Figure 2.4 represents that a significant reduction in horizontal movement is observed for an increase in L/H ratio from 0.5 to 0.7. For a 12m wall, an increase in the L/H ratio from 0.5 to 1.0 brought about a significant reduction in the horizontal movement from 817 mm to 246 mm.

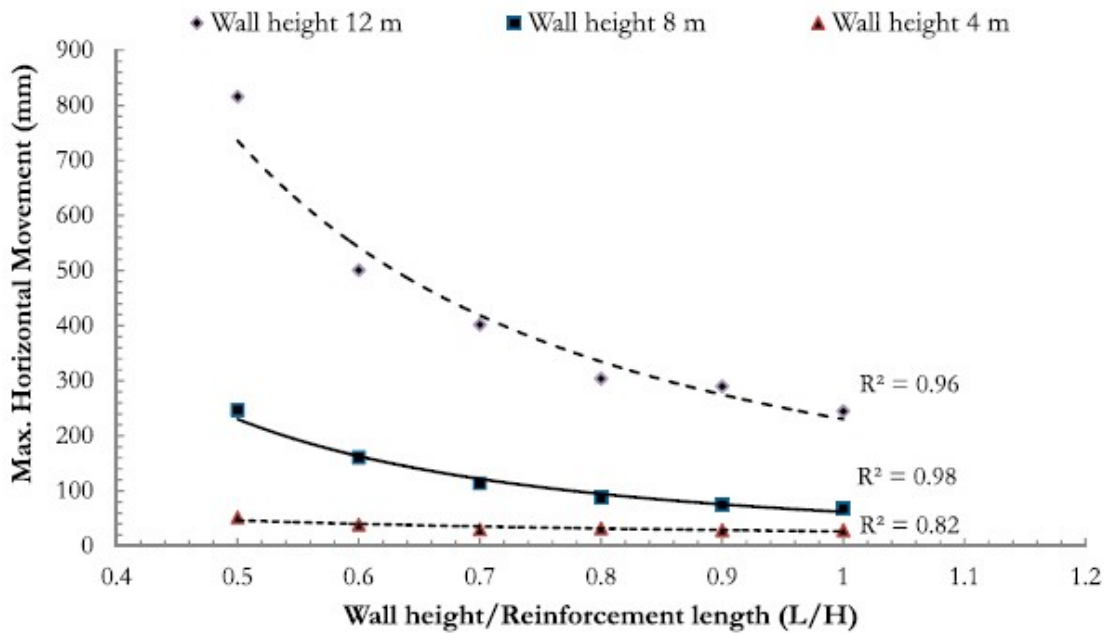


Figure 2.4 Outcome of reinforcement length on horizontal displacement of MSE wall [10]

The effect of reinforcement length on horizontal movement can be attributed to the location of the Rankine failure plane. The author states that a reduction in horizontal movement occurs when the length of the reinforcement extends beyond the Rankine failure plane. Numerical modeling performed under the study concluded that a reduction in horizontal displacement is observed with an increase in reinforcement stiffness, length and backfill soil friction angle at a specified height of the wall.

**Mandal (2014)** concluded that the minimum length of reinforcement (FHWA-NHI-10-024, 2009) for Static Loading as per minimum  $L/H$  ratio = 0.7. He further concluded that the Plasticity Index should not exceed 6 (AASHTO T-90) and the coefficient of uniformity of reinforced fill  $\geq 2$ . Also the maximum spacing ( $S_v$ ) should be 0.5m to 0.6m for geotextile (woven and non-woven) wrapped face walls.

According to a study conducted by **Balakrishnan and Viswanadham (2015)** “Performance evaluation of Geogrid reinforced soil walls with marginal backfills through Centrifuge model tests”, the author states that the selection of a fill type for a particular project depends on various parameters such as strength and deformation requirements,

availability and interaction with reinforcement. Other factors which also attribute in deciding a backfill include grain size, plasticity, and permeability, shear strength and compaction characteristics. The author recommends that the backfill material should be free from organic or deleterious material. To achieve an enhanced soil-reinforcement interaction, the author recommends the use of a well graded and freely draining granular soil. Koerner et al. (1998) recommended a backfill material which is completely free from fines. AASHTO (2009) allows a backfill material with less than 15% of fines passing No. 200 (0.075 mm) sieve and having a plasticity index less than six. Considering the ease of availability, the on-site soil is used in most cases. This result in 20-30% cost reduction, but this soil is marginal and is poorly draining in the literature cited by Mitchell and Zornberg (1995), Koerner et al. (1998), Christopher et al. (1998) and Raisinghani and Viswanadham (2010, 2011). Hence the problems caused by marginal backfill have been a topic of study by the authors.

Centrifuge model test on geogrid soil wall constructed of marginal backfill – weak reinforcement was found to undergo excessive deformations rapidly. Tension cracks were observed right behind the reinforced zone and maximum reinforcement strain was observed at top of the wall. The failure surface was away from the wall facing and observed only in upper half portion of the wall. The author terms the failure, as pullout failure which can be attributed to inadequate soil-geogrid interaction. Another model, constructed of marginal backfill – stronger reinforcement was observed to undergo very limited surface settlements, face movements and peak strains in Geogrid layers. Wide and deep tension cracks were not observed and the failure surface remained close to the wall face. Further, a model was developed with marginal backfill – stronger reinforcement in upper half zone and weaker reinforcement in lower half zone. According to the study, bulging was observed at mid – height, but with limited face movements in the upper half zone. Another observation included deep tension cracks rights behind the reinforced zone. This study involving centrifuge model concludes that provision of stiffer geogrid layers for reinforced soil walls with marginal backfills is one of the viable options to limit the excessive deformations.

A study conducted by **Singh and Akhtar (2015)** puts light on the fact that economics plays a very significant role in the field of civil engineering. The need for constructing more stable and stronger structures with reduction in costs is termed as economical construction. As

of today, we have replaced the metallic reinforcements with geosynthetics and have brought down costs but the fill material continues to be the same. For the present study, the author varied parameters such as height of the wall, backfill material (local earth/ granular sub base/ sand) and reinforcement materials. The study concluded that the major contribution in the cost variation is due to the huge amount of concrete and steel bars utilized in the retaining walls as compared to its counterpart reinforced earth walls. The author further states that there exists a direct relation between the economic benefit achieved from the Reinforced Earth Wall and height of the wall. The percent savings from the reinforced walls may range up to 65%. For the present study, the rates used were as specified in Schedule of rates (SOR) 2014 issued by Madhya Pradesh PWD, India for Roads and Bridges. The comparison of reinforced earth walls with different types of reinforcing elements has been presented in Figure 2.5

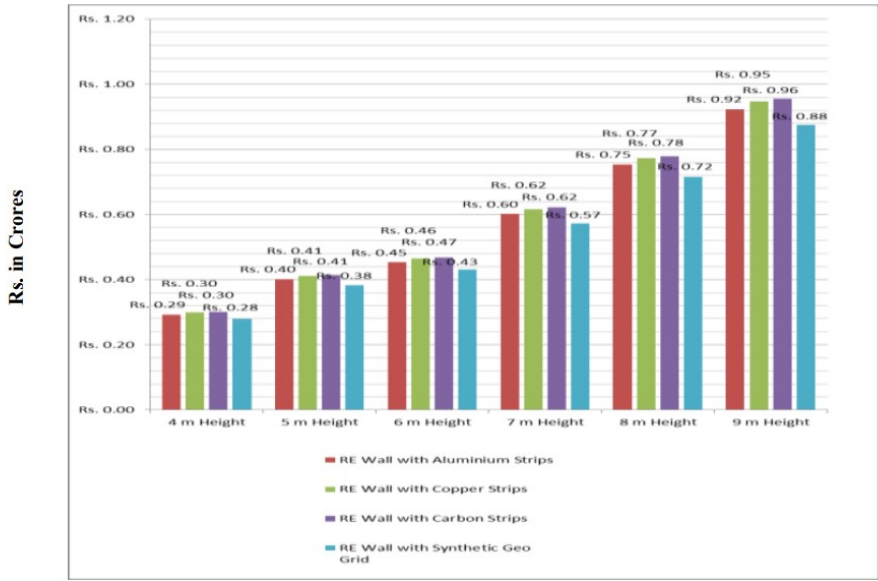


Figure 2.5 Comparison of reinforced earth walls with different types of reinforcing elements [13]

From the cost analysis, conducted in the study, it can be concluded that quantities remaining the same, and only changing the RE wall backfill and reinforcing material, the cost of the reinforced earth wall with geosynthetics turns out to be the most economic with the combination of local earth as backfill material for the reinforced structure.

**Infante et al. (2016)** studies about the shear strength behavior of various geosynthetic reinforced soil structure as obtained from the direct shear test. The author correctly puts forward that the interaction between soil and geosynthetic is of utmost importance for the design, modeling and performance of the reinforced soil structures. Many researches to determine this behavior have been conducted, few have placed the geosynthetic parallel to the shear plane, and while some have placed it perpendicular and the rest have rotated it to the shear plane. In the current study, the geosynthetic layer was placed perpendicular to the failure plane to study the behavior of soil-geosynthetic interaction when they undergo shearing. The ASTM D5321.08 standard suggests that the minimum dimension of the shear box should be 300 mm x 300 mm x 50 mm. But various studies have concluded that the sample size does not affect the results obtained.

### **2.3 Summary of Literature Review**

From the studied literature, it can be summarized that soil reinforcement techniques found their way into the field of civil engineering long ago in the 1960s. From then the technique has evolved, shifting from traditional retaining structures to newer forms of soil reinforcement techniques.

The literature brings to light that a lot of research work has been done on soil stabilization involving geogrids, but there exists a limited amount of work done regarding the behavior of geotextiles in soil stabilization. The study by **Singh and Akhtar (2015)** brings the fact that now; geosynthetics as reinforcement stand more economically viable when compared to the traditional reinforcements. Many of the authors including **Mandal (2014) and Kibria et al. (2014)** stated the increase in load bearing capacity associated with the increase in  $L_{rein}/H$  ratio. The **US Department of Transportation and FHWA (2009)** further put out the fact that increase in  $L/H$  ratio from 0.5 to 0.7, reduces the horizontal deformations by about 50 percent. **Scarborough (2004)** recommends, rather advises to not use a marginal backfill or a backfill having a poor drainage capability, as studies have shown that such reinforced structures have undergone catastrophic failure.

The study by **Krishna and Latha (2012)** is an elaborative study, which includes all the parameters required for physical and numerical modeling mentioned explicitly. The authors have adhered strictly to the IS code for the research and suitably selected parameters for their study. Study of MSE wall under static and dynamic loading has been a field of research for many, which included studying the load-displacement behavior in both, horizontal and vertical directions. A new parameter which is recently been studied, is the strains developed in the geotextile fibers due to the horizontal movement of the structure. The study of the stress-strain curve of the geotextile represents its elastic nature and the ability to undergo deformations before yielding under the maximum tensile force.

## **2.4 Objectives**

From studying the literature and the various case studies and laboratory models, we conclude the following as our objectives for the present study.

1. To investigate the response of mechanically stabilized earth wall with geotextile under compressive load from a footing.
2. To study the strains developed in geotextile under static loading during failure in MSE wall.
3. To validate the model testing by numerical modeling using finite element method.

## CHAPTER 3

### METHODOLOGY

---

#### 3.1 General

In this project a list of certain equipments were used. A model tank of dimension 110 cm x 50cm x 80cm was fabricated for the model to be built in. The geotextile used was woven and made up of polypropylene. On the geotextile surface a 120  $\Omega$  strain gauge was soldered which was further connected to a wheatstone bridge. During the testing of the MSE wall, the wheatstone bridge was supplied with an input potential difference of near about 5V and the corresponding output voltage was measured by a multimeter. Before the final testing on the fabricated model, certain tests were performed on the soil to determine its nature and constituents. The tests involved sieve analysis and direct shear test of the soil.

#### 3.2 Material Used

##### 3.2.1 Woven Polypropylene Geotextile

The geotextile used for wrapping the soil was a multifilament woven polypropylene geotextile. The geotextile used for fabrication is shown in Figure 3.1. Given in Table 3.1 are the specifications of the geotextile as provided by the manufacturer.

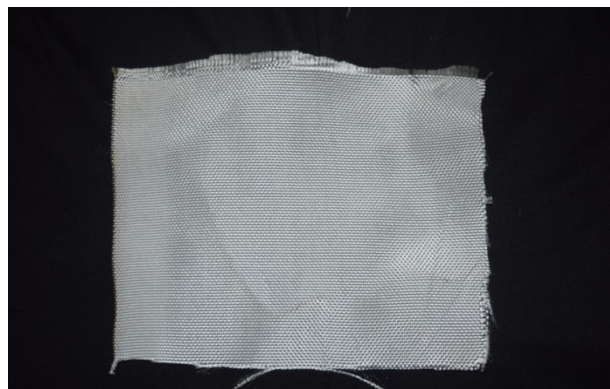


Figure 3.1 Woven Polypropylene Geotextile

Table 3.1: Specifications of Multifilament Woven Polypropylene Geotextile

Property	Particulars	Units	Test Method	Quality No.
				Vt2000
Tensile Strength	WARP	kN/m	IS 1969	45
	WEFT	kN/m	IS 1969	34
Elongation at Break	WARP	%	IS 1969	30
	WEFT	%	IS 1969	28

### 3.2.2 Model Tank

The fabricated model tank has been shown in Figure 3.2 (a) and 3.2 (b). Materials utilized in the fabrication were as follows.

- a) Perspex Sheet – Poly-methyl methacrylate (PMMA), also called as acrylic glass or by its market names, Plexiglass, Lucite, Acrylite and Perspex is a transparent thermoplastic. It is often used in the form of a lightweight or shatter-resistant sheet. It basically functions as an alternative to glass. The same material can be utilized as a casting resin, in inks and finds various other uses. Although it is not a type of a familiar silicate based glass, but like many thermoplastics, is often technically classified as a type of glass. Chemically, this material is the synthetic polymer of methyl methacrylate. The thickness of the Perspex sheet used for the model tank was 6mm.
- b) Iron Angles
- c) Screws



Figure 3.2 (a) Model Tank (Top View)



Figure 3.2 (b) Model Tank (Side View)

### **3.3 Soil Tests**

#### **3.3.1 Sieve Analysis**

Sieve analysis (also known as a graduation test) is a procedure used (commonly in civil engineering) to assess and determine the particle size distribution of a granular material. The size distribution is often of critical importance to the way the material performs in use. A sieve analysis can be performed on any type of non-organic or organic granular materials including sands, crushed rocks, clays, granite, feldspars, coal, a wide range of manufactured powders, grain and seeds, down to a minimum size depending on the exact method. Being such a simple technique of particle sizing, it is probably the most common.

**Procedure:**

Take an oven dried sample of soil that weighs about 1000g. If the soil particles are in the form of lumps or agglomerated, crush the lumps and do not tamper the particles. Determine the mass of the sample accurately using an electronic balance. Prepare the stack of sieves with sieve having a larger opening size placed above the sieves having a smaller opening. A pan is to be placed under the last sieve to collect the soil passing through it.

Table 3.2 Size of sieves used

Sieve Size
10000 $\mu\text{m}$
4750 $\mu\text{m}$
2000 $\mu\text{m}$
1000 $\mu\text{m}$
600 $\mu\text{m}$
425 $\mu\text{m}$
300 $\mu\text{m}$
212 $\mu\text{m}$
150 $\mu\text{m}$
75 $\mu\text{m}$

The list of sieves used has been tabulated in Table 3.2. Make sure that the sieves are clean. If soil particles get stuck in the openings, try to poke them out using a brush. Pour the soil into the stack of sieves from top and place the cover. Put the stack in the sieve shaker and fix the clamps, adjust the time to 10 to 15 minutes start the apparatus. Stop the sieve shaker after sufficient time and measure the mass of soil retained on every sieve.

**3.3.2 Direct Shear Test**

A direct shear test is a basic laboratory test used to measure the shear strength properties of a soil or rock sample. It is also used to study the discontinuities in soil or rock masses.

The test is performed on three to four sample specimens taken from a relatively undisturbed soil sample. The specimen is placed in the shear box. A confining stress is applied vertically to the specimen. The load applied and the strain induced is recorded at regular intervals to plot a stress-strain curve for each individual confining stress. Several specimens are tested at varying confining stresses to determine the shear strength parameters, the soil cohesion ( $c$ ) and the angle of internal friction ( $\phi$ ). The results of the test are plotted on a graph with the shear stress on the Y-axis and the normal stress on the X-axis. The Y-intercept of the curve results in the cohesion value of the soil, and the slope of the line or curve is the friction angle of the soil. If there is no excess pore water pressure generating in the soil sample, the total and effective stresses will be turn out to be identical. From the stresses occurring at failure, the failure envelope can be obtained. The test has several advantages which are listed as follows.

- Direct shear test makes it easy to test sands and gravels.
- If misleading results are being encountered from the test due to fractures and fissures issue, it can be fixed by testing the sample in a large size shear box.
- The sample can be sheared along predetermined planes, when the shear strength along such a plane needs to be determined.

The limitations of the test are listed as follows.

- Failure always occurs at a predetermined horizontal plane, which may or may not be the weakest plane always. Failure of the soil occurs progressively from the edges towards the centre of the sample.
- The direct shear test does not provide any provision to measure the development of pore water pressure. Hence, it is not possible to determine the effective stresses from the undrained tests.
- The side walls cause lateral restraint on the soil specimen and hence do not allow it to deform laterally.

### Direct Shear Test without Geotextile:

#### Procedure:

Note the inner dimensions of the soil container. Put the various components of the soil container together. Place the soil sample in layers (approximately 10mm thick) and tamp the soil. Make the surface of the sample soil plane. Place the upper grating plate and loading block on top of the soil sample. Apply the desired normal load. Remove the shear pin and put in place the sensor (LVDT) which will measure the change. Turn the motor on and take readings of the shear force and corresponding displacement. The direct shear test machine used is shown in Figure 3.7

### Direct Shear Test with Geotextile:

#### Procedure:

Note the inner dimension of the soil container. Assemble the various parts of the soil container together. The geotextile specimen is positioned perpendicular to the failure plane in order to determine the behavior of soil-geotextile system when the shear force acts normal to the reinforcing layer. Make the surface of the sample soil plane. Place the upper grating plate and loading block on top of the soil sample. Apply the desired normal load. Remove the shear pin and put in place the sensor (LVDT) which will measure the change. Turn the motor on and take readings of the shear force and corresponding displacement. A schematic diagram showing the arrangement in case of a direct shear test performed on soil reinforced with geotextile is shown in Figure 3.3. The actual laboratory Figure of the arrangement is depicted in Figure 3.4

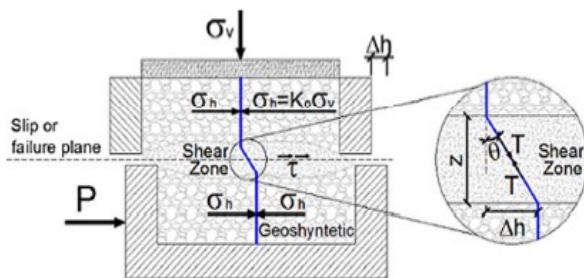


Figure 3.3 Scheme of DST performed

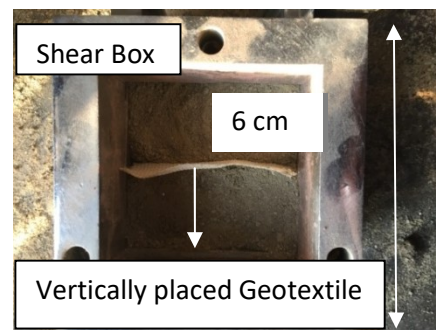


Figure 3.4 Shear Box with Geotextile [14]

### 3.4 MSE Wall Preparation

An MSE wall of dimension 75cm x 50cm x 60cm is to be fabricated and reinforced using woven polypropylene geotextile. The fabricated reinforced wall is to be tested for the above stated objectives.

#### Procedure:

1. The wall is constructed in four layers of 15cm each and subsequent markings for reference are done on the model tank.
2. For model preparation, soil density is decided to be in the range of 15.5 – 16.2 kN/m<sup>3</sup> which is achieved by rainfall technique.
3. First, the base is prepared by spreading soil at the bottom of the model tank to ensure soil – geotextile interaction at the base.
4. Geotextile of length 90cm and width 50cm is chosen for consecutive three layers from the bottom. The geotextile is unrolled and positioned so that approximately 48cm extends over the top of the form and hangs free and the remaining 42cm with strain gauge installed mid-way retains itself on the base soil.
5. Backfill is now placed on the geotextile for  $\frac{1}{2}$  to  $\frac{3}{4}$  of its lift height by making use of the rainfall technique to achieve the desired density.
6. A windrow is made from the face of the wall at a distance of 11cm by digging with hand. Care must be exercised not to damage the underlying geotextile.
7. The free end of the geotextile - that is, its “tail”- is then folded back over the wooden form into the windrow
8. The remaining lift thickness of the soil is then completed to the planned height of 15cm.
9. For the top most layer, geotextile of length 110cm was chosen and the above steps were followed. The model fabrication is presented in Figure 3.5



(a) Placement of Geotextile Layer



(b) Rainfall Technique Apparatus



(c) Fabricated Layer (Front View)



(d) Fabricated Model

Figure 3.5 Various stages of MSE wall fabrication

### 3.5 Instrumentation

#### 3.5.1 Foil Strain Gauges

Foil Strain Gauges are pressure transmitters that are used to detect and measure strain. Foil strain gauges used for our purpose were of  $120\Omega$ . These strain gauges form a part of the wheatstone bridge and help in measuring the strain with the help of a multimeter. For this purpose, a foil strain gauge was mounted on every layer of geotextile, preferably at soil-geotextile interaction. The strain gauge was soldered with copper wires. The basal size was  $6.6\text{mm} \times 3.2\text{mm}$ . The wire grid size was  $3\text{mm} \times 2.3\text{mm}$  and the basal material was Phenolic-Epoxy-Acetal. The nominal tolerance of the strain gauge was less than equal to  $3\Omega$ . The foil strain gauge is shown in the Figure 3.6

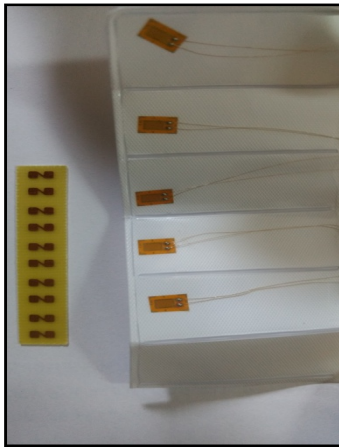


Figure 3.6 Foil Strain Gauge



Figure 3.7 Digital Multimeter

### 3.5.2 Digital Multimeter

A digital multimeter is a tool used to measure two or more electrical values – principally voltage (volts), resistance (ohms) and current (amps). It is a standard tool for technicians, used widely in the electrical and electronic industry.

Digital multimeters have replaced the trivial needle-based analog meters due to their ability to measure with greater accuracy, reliability and increased impedance. Digital multimeters combine the testing capabilities of single-task-meters – the voltmeter, ammeter and ohmmeter. They often have a number of additional specialized features. Technicians seeking specific functions can therefore use a particular model for particular tasks. We used DT830D Digital Multimeter (Figure 3.7) for measuring the voltage in mV. The face of a digital multimeter typically includes four components:

- Display: To view the measurements.
- Buttons: For switching between various functions, the options vary by model.
- Dial: For selecting primary measurement values (volts, amps, ohms).
- Input Jacks: Input slot for test leads.

### 3.5.3 Wheatstone Bridge

A wheatstone bridge is an electrical setup used to measure an unknown electrical resistance by balancing the two legs of a bridge circuit, one leg of which includes the unknown component. The wheatstone bridge is highly sensitive and hence delivers extremely accurate results. Its operation equation is cited below.

$$\frac{R1}{R2} = \frac{R3}{R4}$$

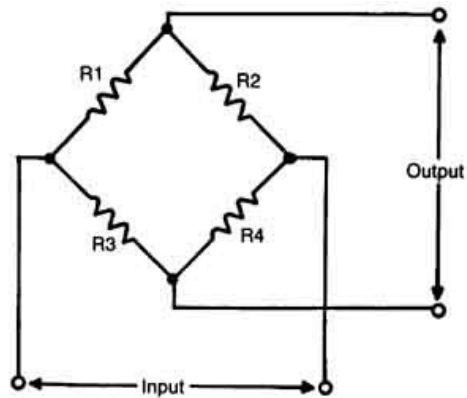


Figure 3.8 Wheatstone Bridge Circuit

### 3.5.4 Connecting Wires

Copper wires were used to establish connections in the wheatstone bridge circuit. The diameter of the wires used was 1mm.



Figure 3.9 Connecting Wires

### Procedure for Model Testing:

Strain gauges were installed at the middle of the geotextile sheet which forms the bottom part of each subsequent layer. These strain gauges are soldered with wires. Each strain gauge is connected to an individual wheatstone bridge. Each wheatstone bridge is supplied with an input voltage of about 5V. The load is applied by using a hydraulic jack resting on a surcharge plate, made of iron (75cm x 50cm) to ensure uniform loading takes place.

As there is an increase in the load applied, the resistance developed in the strain gauge changes which is measured by recording the  $V_{out}$  across the terminals of the wheatstone bridge as shown in Figure 3.10 (b) and 3.10 (c). The circuit diagram for measuring the input and an output voltage is presented in Figure 3.10 (a). The relation between the voltage and resistance of a wheatstone bridge is given by the following equation.

$$\frac{V_{out}}{V_{in}} = \frac{R_3}{R_3 + R_g} - \left( \frac{R_2}{R_2 + R_1} \right) \quad (1)$$

$V_{in}$  – Input voltage

$R_1, R_2, R_3$  – Arms of wheatstone bridge

$R_g$  – Resistance of strain gauge

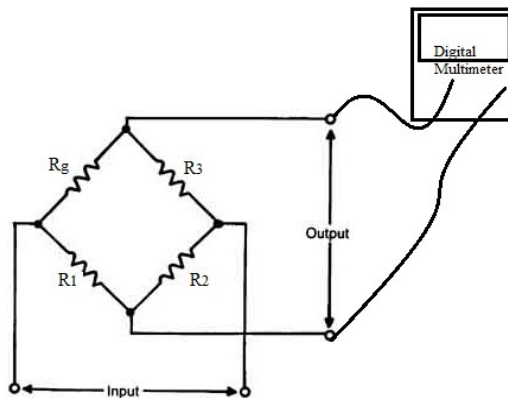


Figure 3.10 (a) Setup of the wheatstone bridge circuit

Now the obtained resistance value is used to calculate the strain value developed in the geotextile by the formula:

$$\epsilon = \frac{\frac{\Delta R}{R}}{GF} \quad (2)$$

$\Delta R$  – Change in resistance

$R$  – Initial resistance of strain gauge

$GF$  – Gauge Factor

$\epsilon$  – Developed strain in geotextile

From the recorded output voltage and provided input voltage and known resistors  $R_1$ ,  $R_2$ ,  $R_3$ , gauge resistance  $R_g$  is calculated by the formula given in equation 1. From these recorded values of  $R_g$ , change in resistance is calculated, and from this value strain in the geotextile is calculated by the formula given in equation (2).

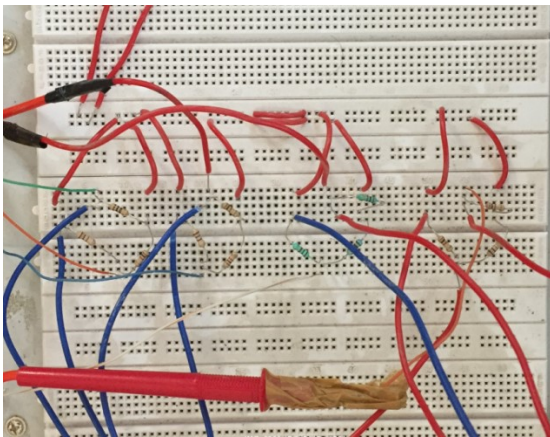


Figure 3.10 (b) Project board



Figure 3.10 (c) Digital Multimeters to measure  $V_{out}$

The value of the resistors used as components of the wheatstone bridge and the input voltage provided for each individual circuit has been tabulated in Table 3.3

Table 3.3 Resistance of arms of four wheatstone bridge

Resistance Arms	1 <sup>ST</sup>	2 <sup>ND</sup>	3 <sup>RD</sup>
R <sub>1</sub>	88.5Ω	86.2 Ω	88.5 Ω
R <sub>2</sub>	86.2 Ω	85 Ω	86.2 Ω
R <sub>3</sub>	86 Ω	86.5 Ω	86.1 Ω
Input Voltage	5.10V	5.04V	5.08V

### 3.6 Model Testing

Our fabricated model of MSE wall was tested by applying uniform load with the help of a hydraulic jack in contact with a surcharge plate. The uniform loading was done in regular intervals in order to give ample time for the various values being noted to become constant. The model proposed to be fabricated and the actual model fabricated has been depicted in Figure 3.11 and Figure 3.12. Following readings were noted and their corresponding graphs have been plotted.

- Horizontal Displacement at a height of 22cm from base – Layer 1
- Horizontal Displacement at a height of 35cm from base – Layer 2
- Horizontal Displacement at a height of 50cm from base – Layer 3
- Vertical Displacement.
- Strains developed in all the layers at the point of soil-geotextile interaction.

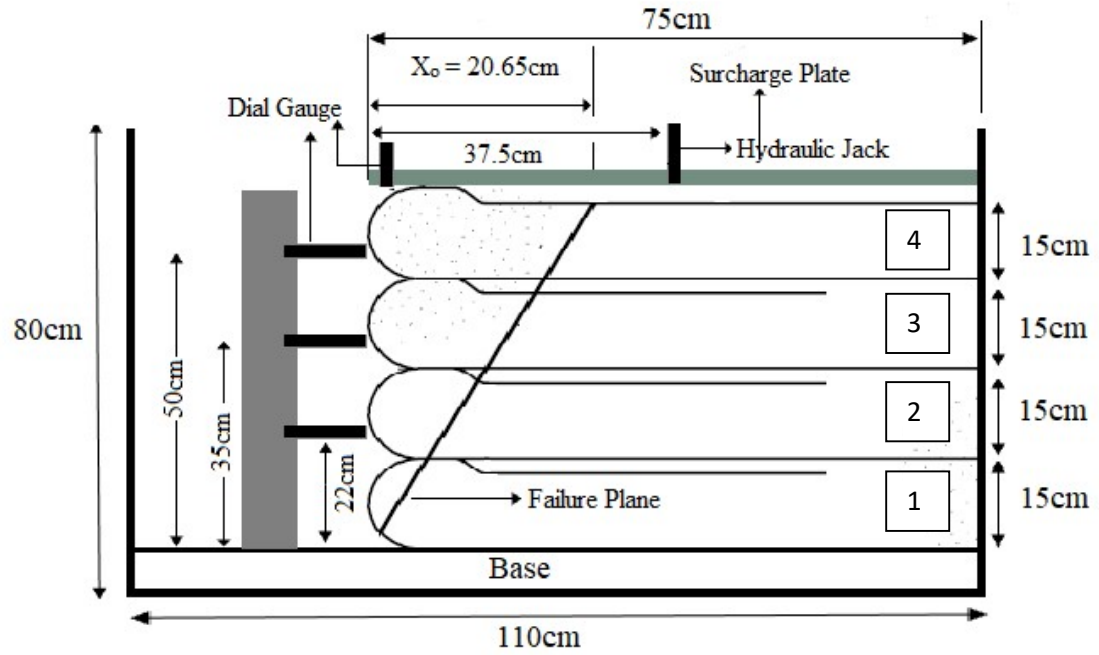


Figure 3.11 Schematic Diagram for completed setup of MSE Wall

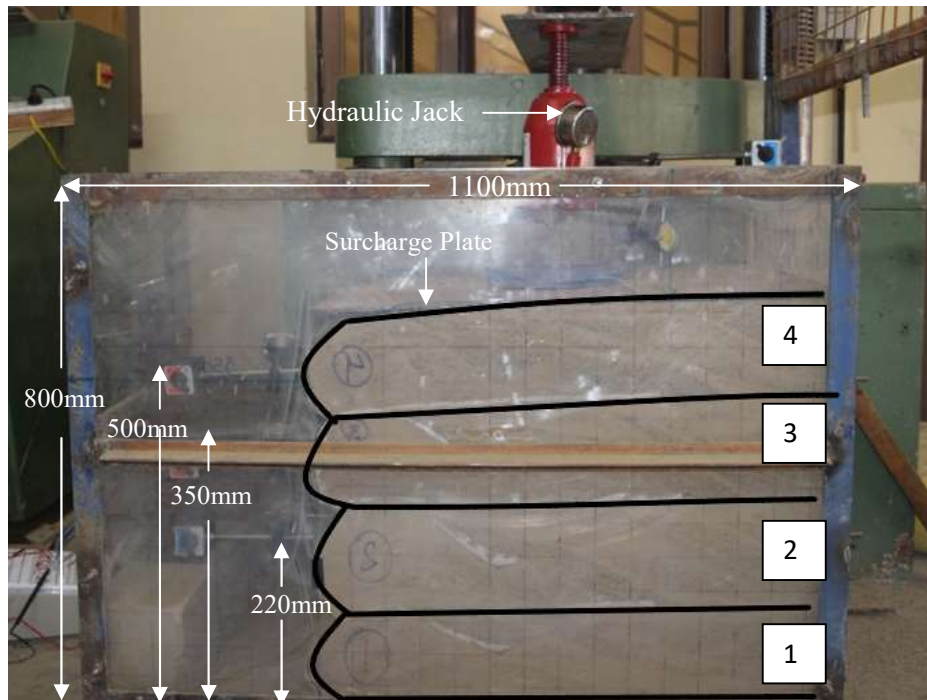


Figure 3.12 Fabricated Model

## CHAPTER 4

# NUMERICAL MODELING

---

### 4.1 General

Generally, there exist two branches of analysis that are utilized in the industry; 2-D modeling and 3-D modeling respectively. 2-D modeling is a simple process and does not need a high end processor. The 2-D modeling tends to yield less accurate results as compared to 3-D modeling. On the other hand, 3-D modeling delivers much more accurate results but requires a high-end processor for the computation. The software used for the analysis and validation of the MSEW is Plaxis-2D.

Plaxis-2D is a finite element package used for two-dimensional analysis of deformation and stability in geotechnical engineering and rock mechanics. A wide variety of geotechnical problems are analyzed with the help of this software. PLAXIS 2D has been developed as advanced and extended package, including advanced soil models, static elastoplastic deformation,, stability analysis, consolidation, updated mesh analysis and steady-state groundwater flow.

For the purpose of evaluating our model using a finite analysis, a finite element mesh was created, material properties of soil and geotextile specified. After specifying the initial parameters, the boundary conditions need to be specified. To develop a finite element model, a 2-D geometry model was created positioned in the XY-plane. Based on the input provided, appropriate finite element mesh, material properties and boundary conditions are automatically performed by the PLAXIS at an elementary level. The final part of a series of inputs involves the generation of pore water pressure and initial effective stresses. For our consideration, there was no generation of pore water pressure.

## 4.2 Material Properties

For a first request estimate of the genuine soil conduct, the Mohr-Coulomb display has been chosen as the material model. For our thought, the model requires 5 input parameters, in particular, Young's modulus  $E$ , Poisson's proportion  $\nu$ , cohesion  $c$ , friction angle of soil  $\phi$ , and a dialatancy angle  $\psi$ . While reproducing the drained behavior, no excess pore water pressures were produced, which is essentially our case.

The saturated and unsaturated unit weights, strength parameters of the soil are determined in the lab. The values obtained from the laboratory testing are used for the input in the numerical modeling. In case of Poisson's ratio and dialatancy angle, standard values for sand have been used. The soil parameters have been presented in Table 4.1

Table 4.1 Material Properties Used in Numerical Modeling

<b>Soil Properties</b>	
Mass Density, $\text{kg/m}^3$	1.63
Poisson's Ratio ( $\nu$ )	0.300
Friction angle ( $\phi$ ), degrees	30
Dilation angle ( $\psi$ ), degrees	0
Cohesion, $\text{kg/cm}^2$	0.07
Young's Modulus, $\text{kN/m}^2$	50,000
$\gamma_{unsat}$ , $\text{kN/m}^3$	15.8
$\gamma_{sat}$ , $\text{kN/m}^3$	18
Interface Strength ( $R_{inter}$ )	0.945
<b>Reinforcement (Geotextile) Properties</b>	
Mass per unit area, $\text{g/m}^2$	200
Stiffness, $\text{kN/m}$	150
Modulus of Elasticity ( $E$ ), $\text{kN/m}^2$	150,000
Tensile Yield Strength ( $N_p$ ), $\text{kN/m}$	45
EA, $\text{kN/m}$	75,000

Reinforcement (geotextile) was modeled using the “geogrid” element. The geogrid element possesses only one (axial) degree of freedom at each node, and is subjected to tensile forces only. Geotextile properties used for modeling the geogrid have been tabulated in Table 4.1

Every interface has allotted to it a 'virtual thickness' which is a fanciful measurement used to characterize the material properties of the interface. The roughness of the interaction is modeled by choosing a suitable value for the strength reduction factor in the interface ( $R_{inter}$ ). For our analysis, value of  $R_{inter}$  has been chosen as 0.945 (Table 4.1)

### 4.3 Model Configuration

The configured model used for the analysis is as presented in Figure 4.1. The model is indicative of the geometry and boundary conditions as simulated in the analysis.

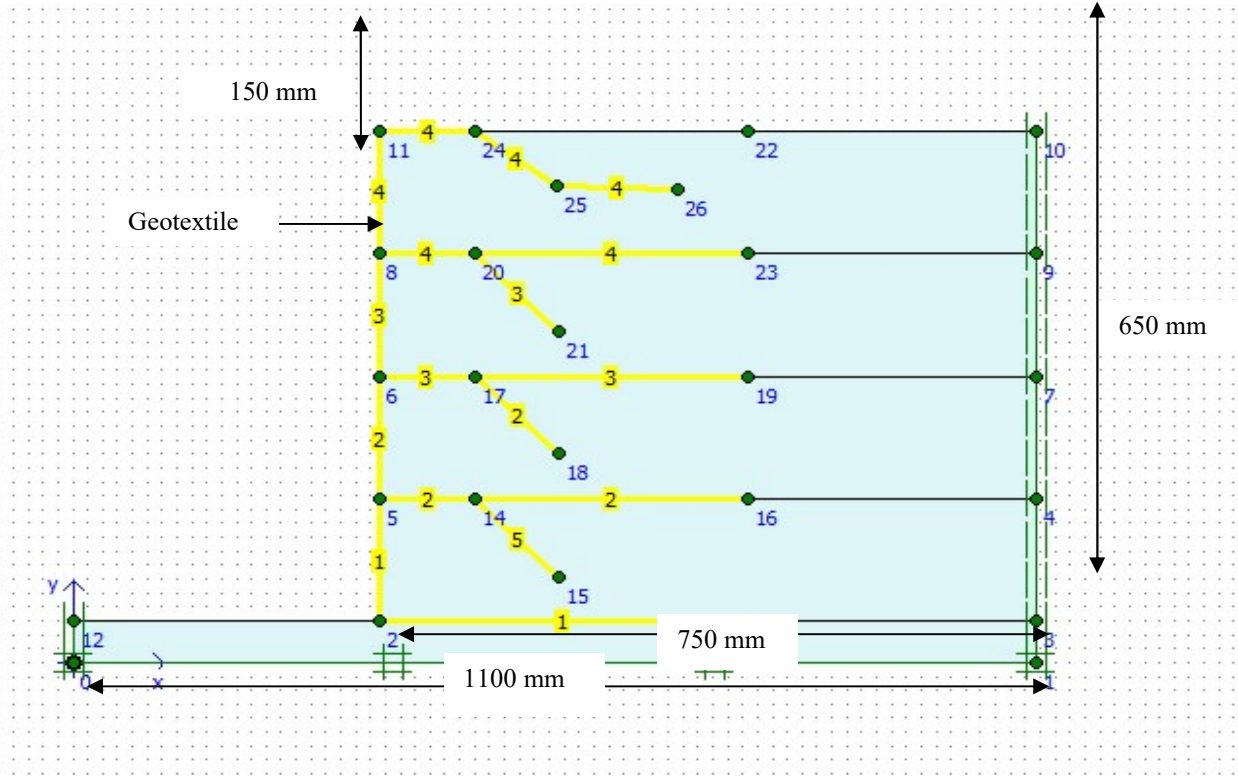


Figure 4.1 Geometry Model with all structural elements

## 4.4 Mesh Generation

Once the geometry of the model is completely characterized and material properties assigned, there occurs a need to divide the geometry into finite elements in order to permit finite element calculations. The organization of finite elements is called a mesh. Plaxis 8.0 permits fully automatic mesh generation in majorly these forms – very coarse, coarse, medium, fine and very fine.

The vertical and horizontal boundaries were considered to be fixed in their respective directions. The stability of the foundation soil does not form a part of this analysis and therefore the bottom boundary of the model has been simulated as a fixed boundary. Figure 4.2 represents the generated mesh.

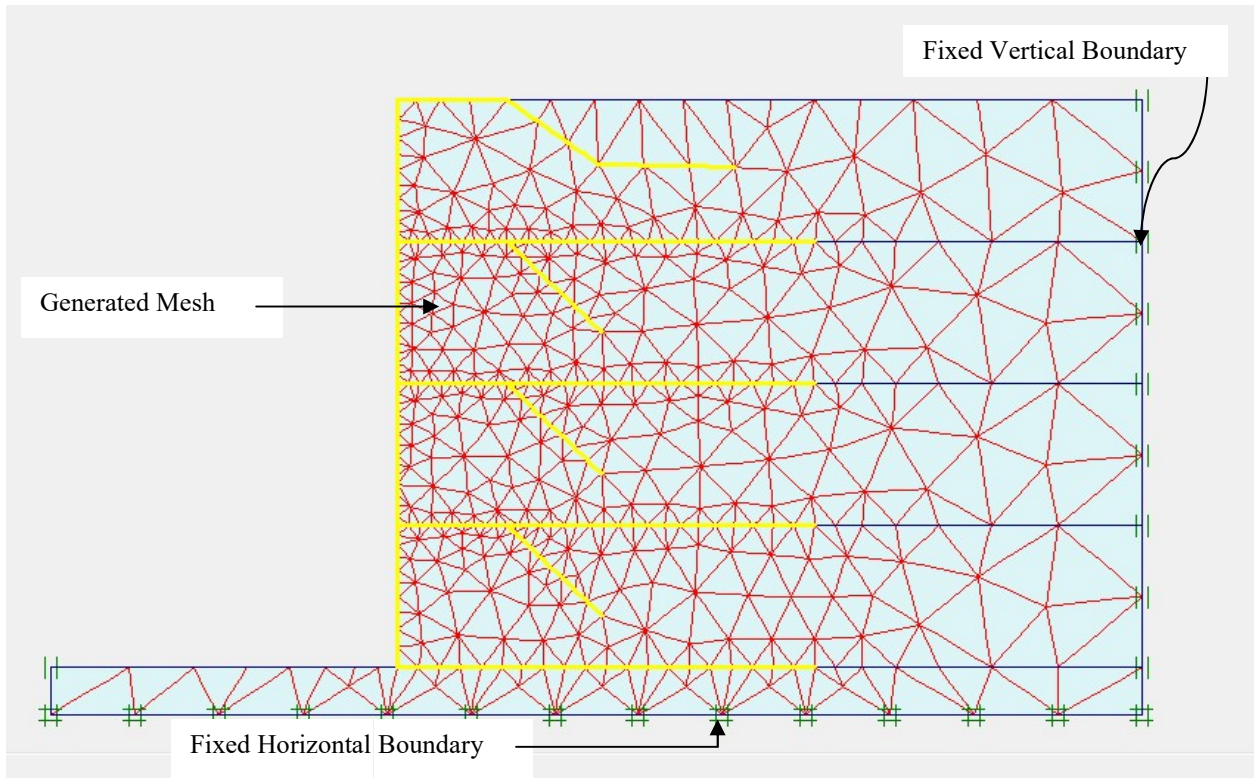


Figure 4.2 Generated Mesh at initial condition

## 4.5 Initial Stress Distribution and Loading

The parameters affecting the initial stress of a soil mass are its own weight and history of soil formation. In Plaxis, the effective initial stress is analyzed by the  $K_0$  (at rest) condition. The initial stresses simulated are presented in Figure 4.3

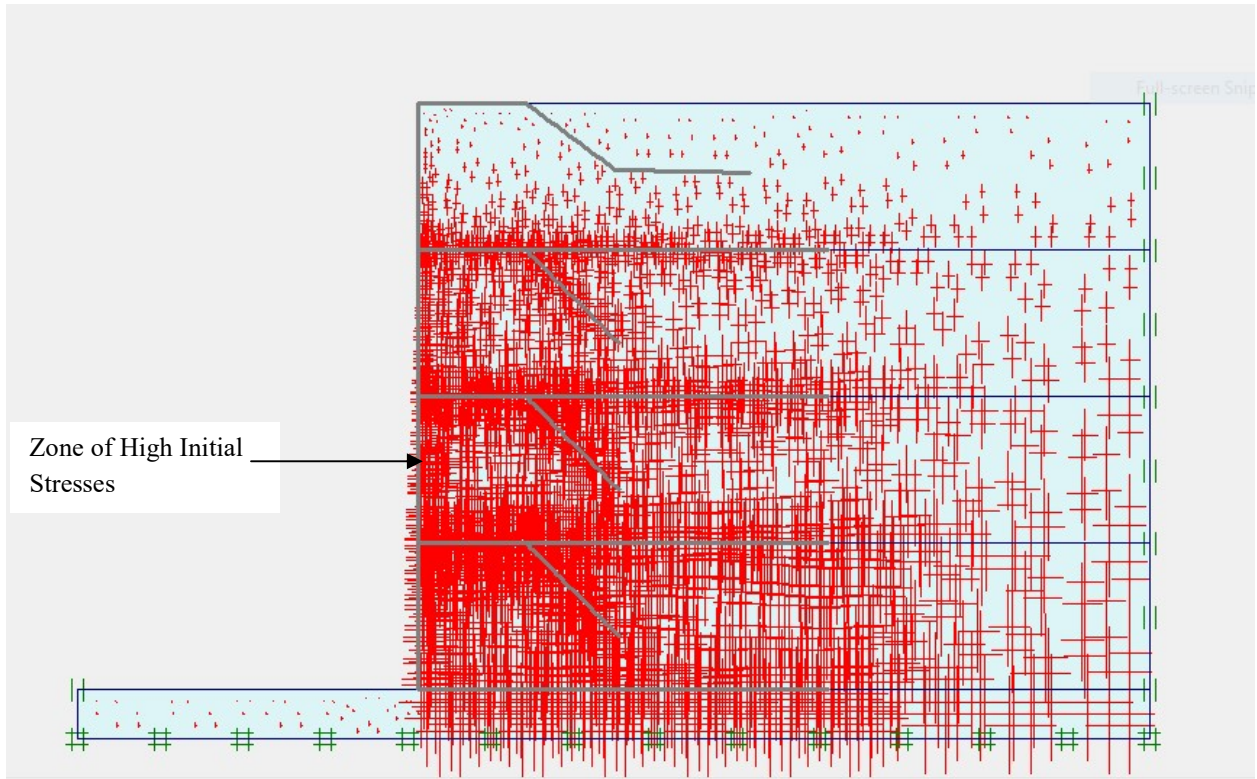


Figure 4.3 Effective Stresses Distribution

Due to the presence of this overburden pressure, the soil mass undergoes a smaller degree of initial compression, which consequently results into the horizontal movement of the wall. The movement of the wall, as analyzed by Plaxis, results into a maximum total displacement of  $28.19 \times 10^{-3}$  mm. This initial horizontal movement is presented in Figure 4.4

A uniform distributed load was applied to the simulated model. The loading is presented in Figure 4.5. With this step, the modeling of the MSE wall and subsequent simulation reaches its end. The next step involves obtaining the results and analyzing them.

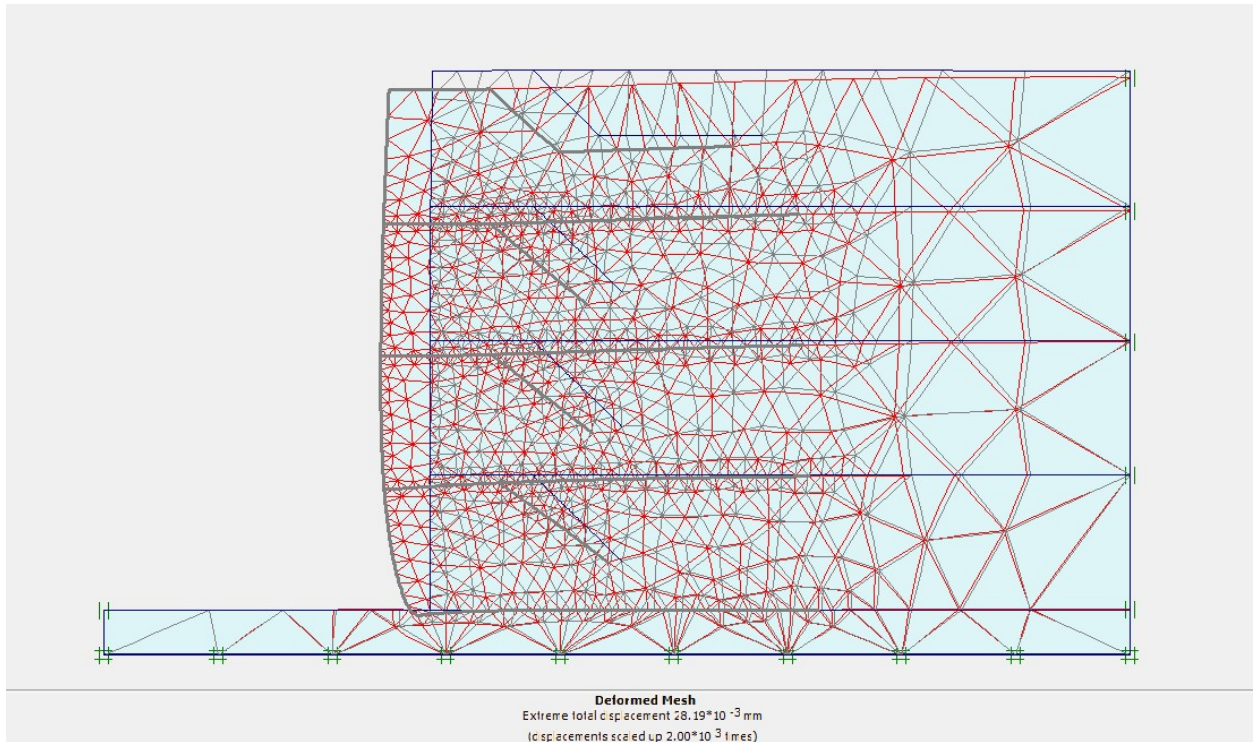


Figure 4.4 Deformed Mesh under Overburden Pressure

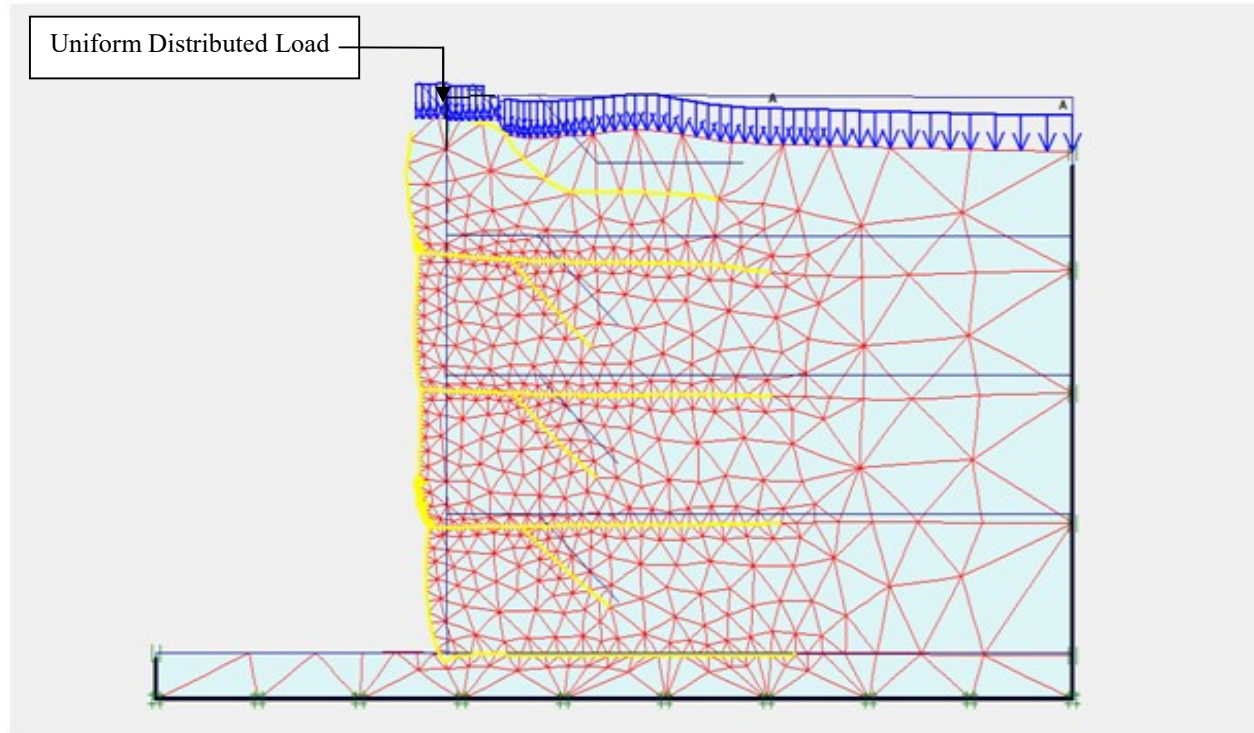


Figure 4.5 Application of Uniform Distributed Load

### 5.1 General

Experimentation on soil reinforcing techniques to obtain the maximum strength and stability by varying various parameters like the backfill material, reinforcement material - spunbonded, needle punched, nonwoven, woven, polypropylene / polyester geotextiles and the  $L_{rein} / H$  ratio have been done in the past by various researchers.

We continued this experimentation on soil reinforcing techniques with an aim of determining the maximum deflections corresponding to maximum load in both directions, horizontal as well as vertical. We also aim to establish the relation between the strain developed in each layer of geotextile fabrication and the corresponding loads imposed. After conducting the modeling, followed by testing, the following things could be concluded.

### 5.2 Laboratory Results and Discussions

Sieve analysis and direct shear test are the tests which were conducted on the backfill soil specimen and the results obtained from the above tests are mentioned and discussed in the following section.

#### 5.2.1 Sieve Analysis

Sieve analysis was conducted in order to obtain the particle size distribution of soil sample. With the help of this data, we can classify our soil based on its grain size. Readings obtained from sieve analysis are displayed in Table 5.1 and its graphical representation is shown in Figure 5.1. Particles having a grain size less than 0.002 mm are classified as clays, those ranging from 0.002mm to 0.05mm are classified as silt, from 0.05mm to 0.10mm are classified as fine sand, 0.25mm to 0.50mm are classified as medium sand and 0.50mm to 2mm are coarse sand.

Table 5.1 Particle Size Distribution Table

Sieve Size (mm)	Weight retained (gm)	Percentage Retained	Cumulative Retained	Percentage Finer
10	2.6	0.26	0.26	99.74
4.75	16.6	1.66	1.92	98.08
2	271.2	27.12	29.04	70.96
1	395.1	39.51	68.55	31.45
0.6	146.7	14.67	83.22	16.78
0.425	80.2	8.02	91.24	8.76
0.3	7.6	0.76	92	8
0.212	33.5	3.35	95.35	4.65
0.15	8.1	0.81	96.16	3.84
0.075	16.8	1.68	97.84	2.16
Pan	19.5	1.95	99.79	0.21

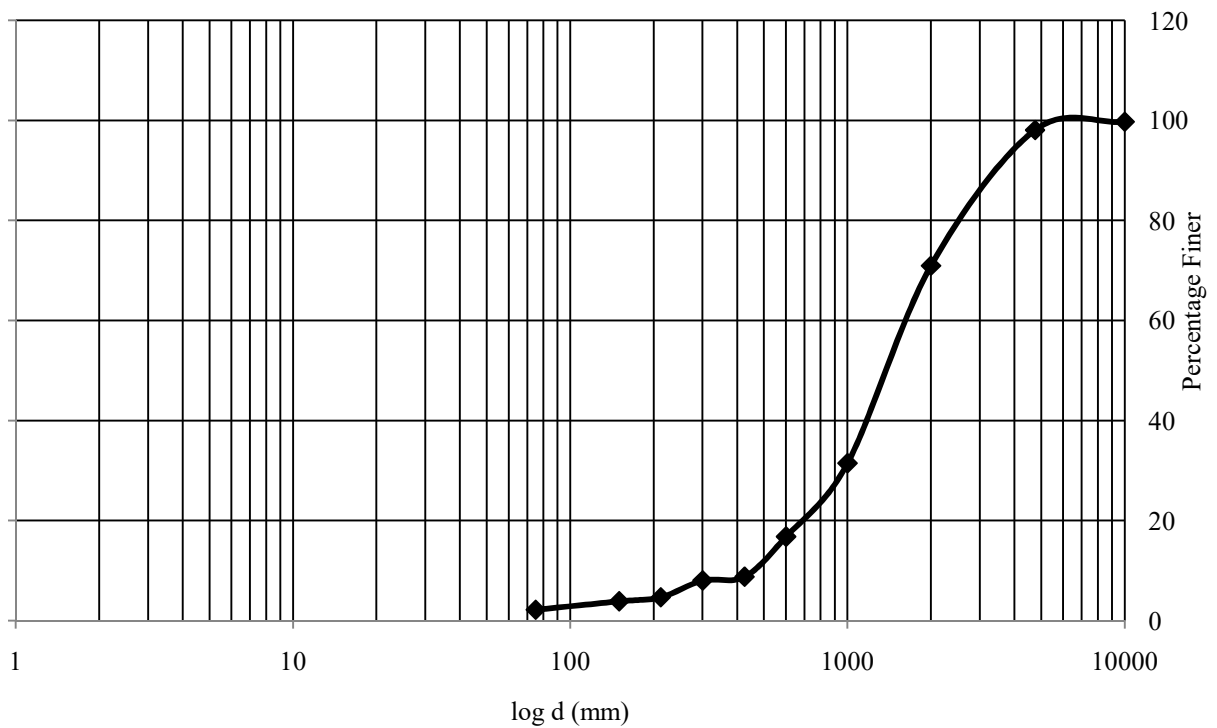


Figure 5.1 Particle Size Distribution Curve

**Result:** From the above graph, it can be concluded that the soil specimen is poorly graded sand.

## 5.2.2 Direct Shear Test

To obtain the strength parameters of the soil specimen, direct shear test was conducted on the soil specimen, and for this purpose two distinct soil samples were prepared, first with dry soil and the second prepared was soil sample reinforced with geotextile.

### 5.2.2.1 Dry Soil Sample

Direct shear test was performed on the soil specimen. The results obtained have been tabulated (Table 5.2) and the corresponding graph between shear stress and normal stress has been plotted as shown in Figure 5.2

Table 5.2 Values of Normal Stress and Shear Stress

	Normal Stress	Shear Stress
Sample 1	0.2 kg/cm <sup>2</sup>	0.12665 kg/cm <sup>2</sup>
Sample 2	0.4 kg/cm <sup>2</sup>	0.18754 kg/cm <sup>2</sup>
Sample 3	0.8 kg/cm <sup>2</sup>	0.21467 kg/cm <sup>2</sup>

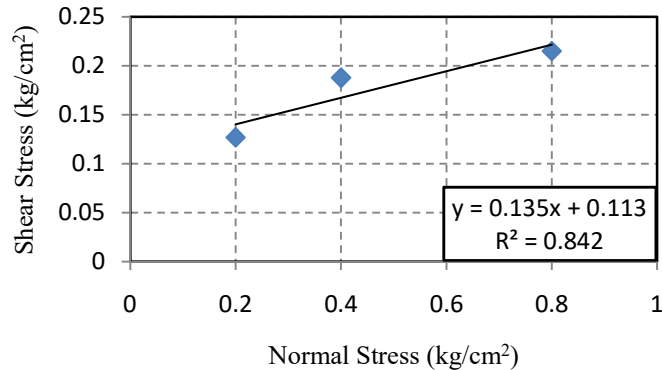


Figure 5.2 Variation of Normal Stress and Shear Stress

**Result** – After conducting the experiment, the following values of  $c$  and  $\phi$  were obtained –

- $c$  value = .07 kg/cm<sup>2</sup>
- $\phi$  value = 30°

These values of  $c$  and  $\phi$  shows that our soil is mostly sand as the cohesion value is quite less.

### 5.2.2.2 Dry Soil Sample reinforced with Geotextile

Direct shear test on the soil sample reinforced with geotextile is an important test to check and study the degree of change in soil strength parameters,  $c$  and  $\phi$  respectively. The results obtained have been tabulated (Table 5.3) and the corresponding graph between shear stress and normal stress has been plotted as shown in Figure 5.3

Table 5.3 Values of Normal Stress and Shear Stress

	Normal Stress	Shear Stress
Sample 1	0.2 kg/cm <sup>2</sup>	0.32015 kg/cm <sup>2</sup>
Sample 2	0.4 kg/cm <sup>2</sup>	0.56823 kg/cm <sup>2</sup>
Sample 3	0.8 kg/cm <sup>2</sup>	0.59510 kg/cm <sup>2</sup>

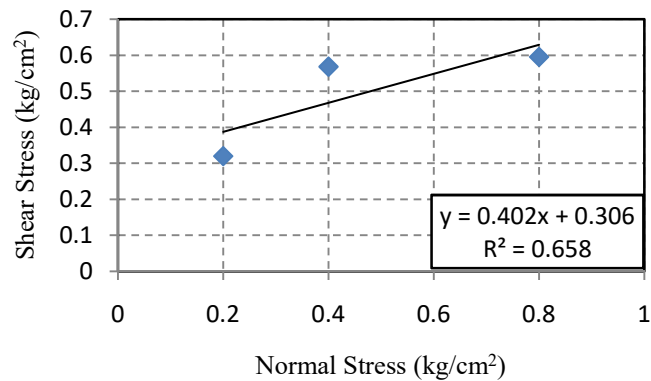


Figure 5.3 Variation of Normal Stress and Shear Stress

**Result** – After conducting the experiment, the following values of  $c$  and  $\phi$  were obtained –

- $c$  value = .07 kg/cm<sup>2</sup>
- $\phi$  value = 52°

These values of  $c$  and  $\phi$  bring out the fact that reinforcement with geotextile does not increase the cohesion but certainly increases the angle of friction, as expected. This increase in angle of friction leads to establishment of a much more reinforced and stable soil mass.

### 5.3 Load-Displacement under Footing

As specified in the methodology, the variation of horizontal and vertical displacement with the applied pressure has been plotted and represented in Figure 5.4 and 5.5.

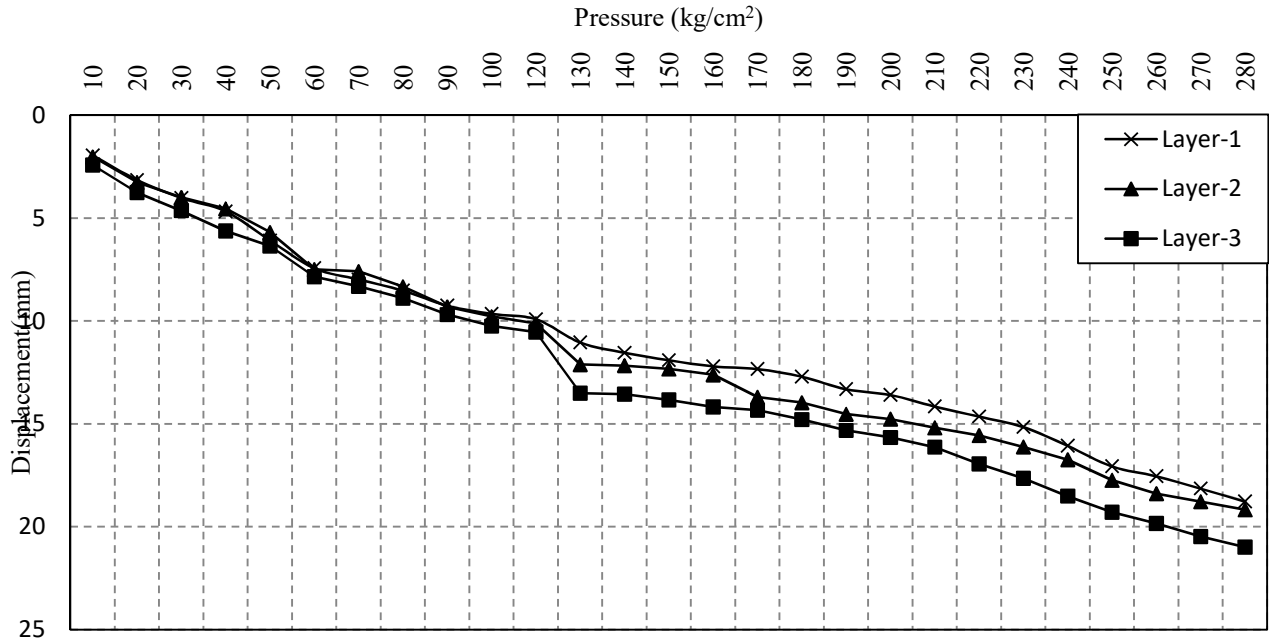


Figure 5.4 Variation of Horizontal Displacement vs. Pressure

From Figure 5.4, it can be observed that the fabricated MSE wall undergoes a nominal horizontal displacement as the load applied is less in magnitude coupled with rearrangement of soil particles. With further increase in the magnitude of load, there occurs a gradual increase in the graph corresponding to increase in horizontal displacement due to the decrease in the number of voids which initiates the compression of the soil mass. With further increase in load and subsequent compression reaching its limiting value, there is a sudden increase in the horizontal displacement which is followed by densification of soil leading to a slow increase in the horizontal displacement. The pattern followed by the variation of horizontal displacement and pressure applied is being imitated in the case of variation of vertical displacement with the pressure. The plot of variation of vertical displacement with pressure is represented in Figure 5.5

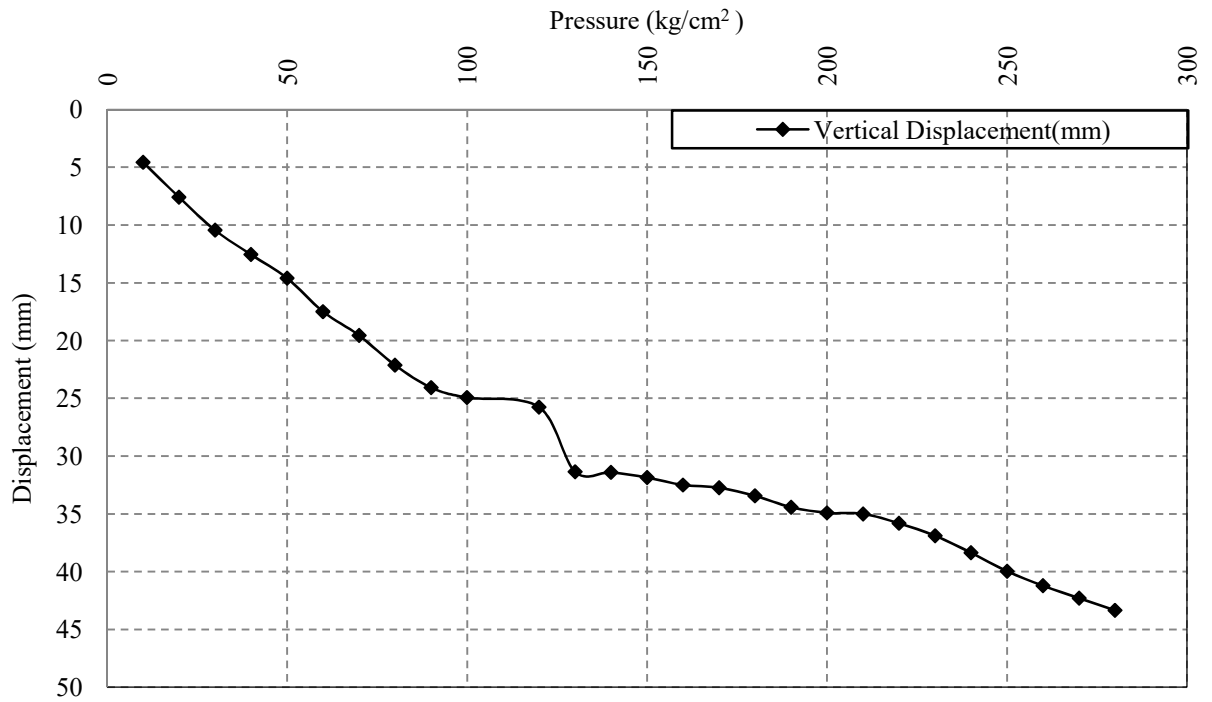


Figure 5.5 Vertical Displacement of MSE under footing

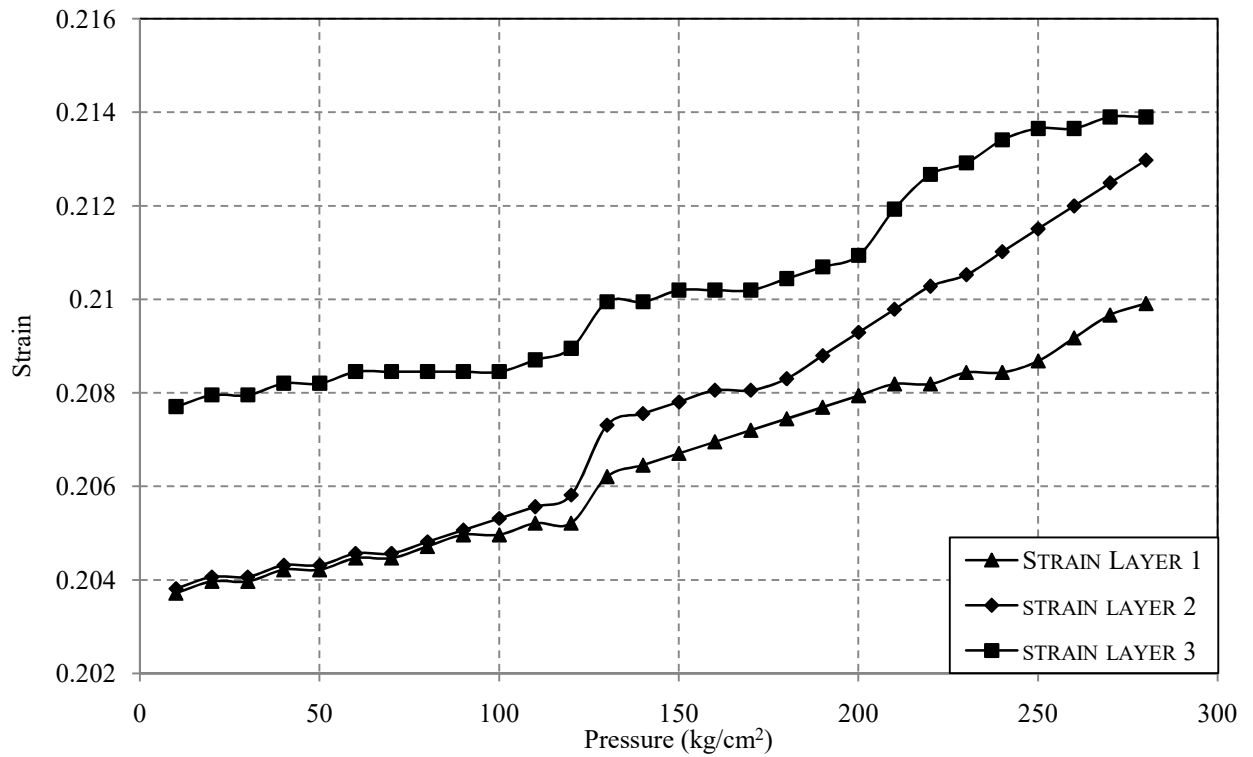


Figure 5.6 Variation of Strain vs. Pressure

Equation (1) and (2) were solved considering the resistances provided by the arms of the wheatstone bridge and the input voltages. The values obtained for strains in the different layers were plotted against the applied pressure. The graph obtained is represented in Figure 5.6. The mismatch observed in the initial position of Layer 1, 2 and Layer 3 can be attributed to the horizontal movement of that definite point during construction of the MSE wall. The maximum values of strain are observed in the topmost layer, that is, Strain Layer -3. This finding can be attributed to the extension caused in the Geotextiles. Since the 3<sup>rd</sup> layer undergoes a larger magnitude of horizontal displacement as depicted in Figure 5.4, this contributes to the reason of it being subjected to a larger strain value.

## **5.4 Results from Numerical Modeling**

The MSE wall numerical model simulated according to various parameters was modeled and run on Plaxis 2D. The results obtained were compiled, plotted and presented in the following section. The analysis utilizing Plaxis 2D gives an insight into stress distribution across the model, the axial forces developed in the reinforcement, displacement of the reinforcement, the plastic points and the failure surface.

### **5.4.1 Displacements**

Figure 5.7 represents shows the total displacement pattern in the MSE wall. The direction and magnitude of displacement is marked by the red arrow and the length of the arrows, respectively. From Figure 5.7 maximum displacement is recorded at top face of the wall with a value of 39.55mm.

Figure 5.8 represents the displacement contours in soil. Each color of the plot corresponds to a range of displacement, given at the right of the plot in the form of a legend. The maximum displacement is observed in the red zone. As the displacement decreases, the color changes from red to blue, with blue signifying the zone of no or zero displacement.

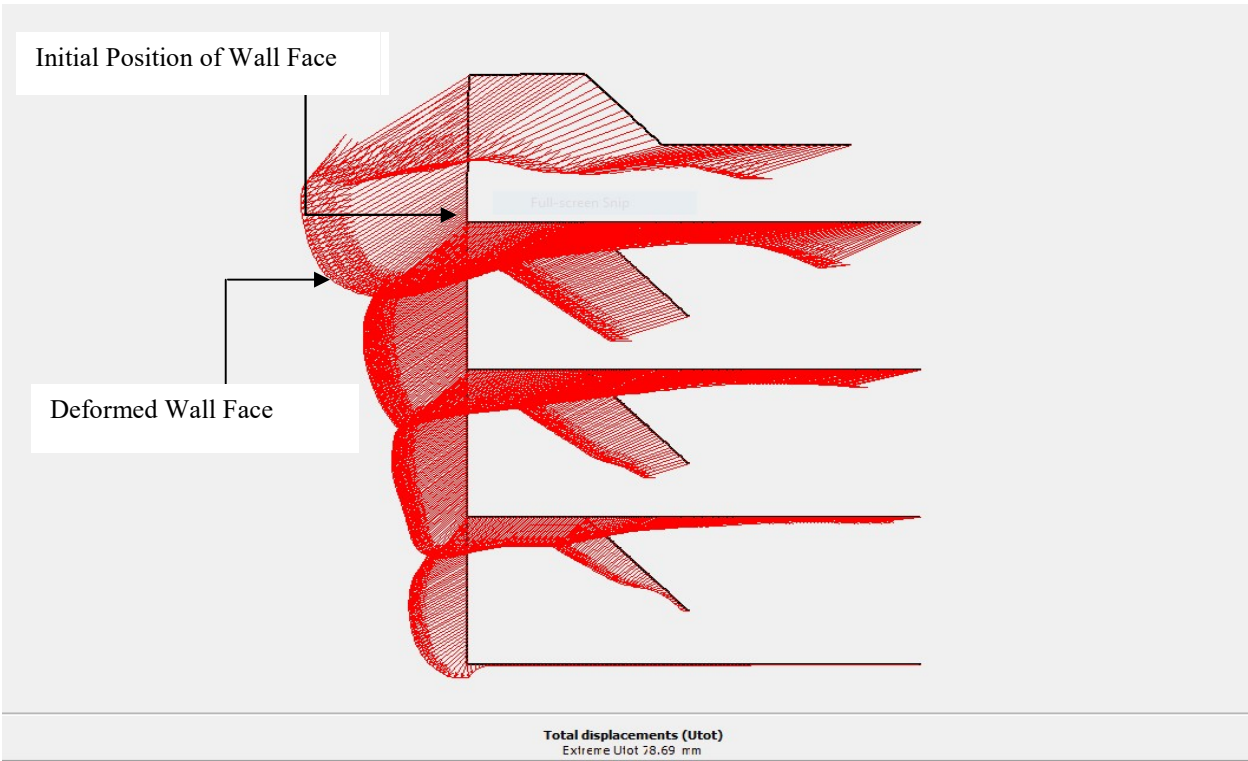


Figure 5.7 Displacement of Geotextile

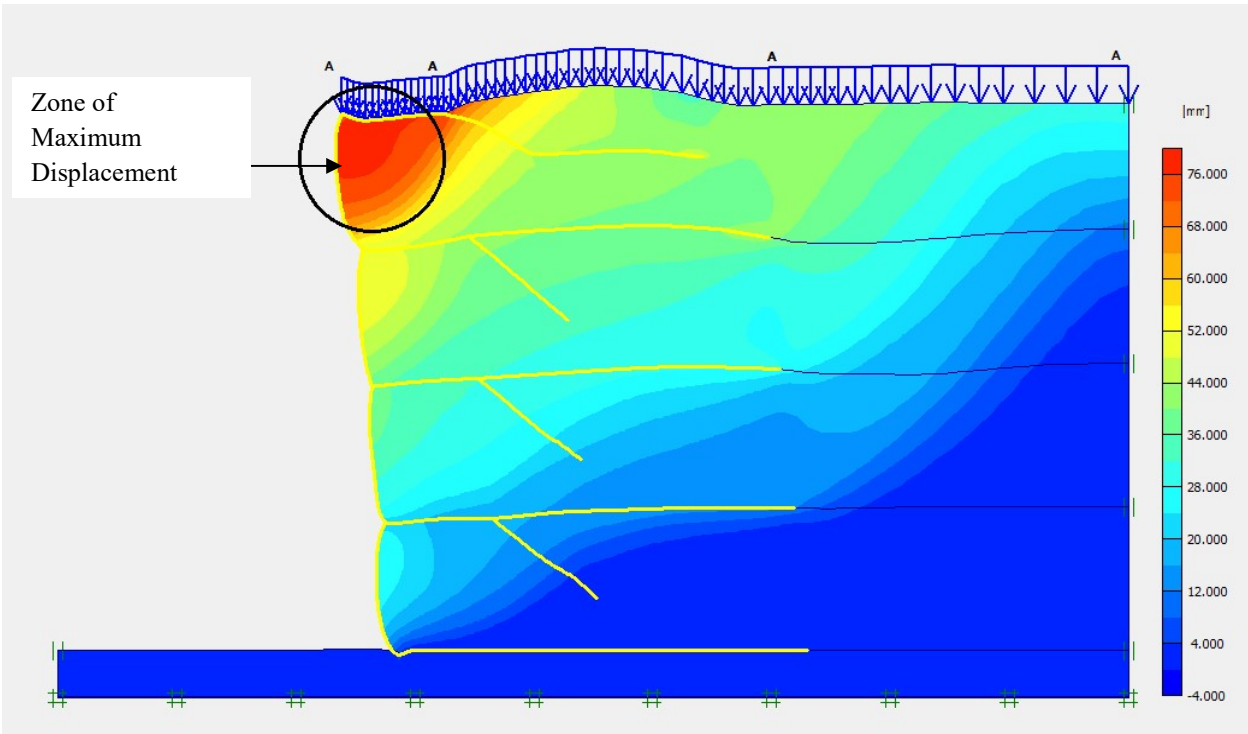


Figure 5.8 Displacement Contours

### 5.4.2 Stresses

The mean effective stress distribution is presented in 5.9. The highest mean stress,  $-1180 \text{ kN/m}^2$  is observed at the foundation of the MSE wall. During the displacement of wall, the soil pressure at foundation level increases due to soil movement away from the wall. Therefore, there is possibility of increase in effective stress at foundation level, which is reflected here during the numerical modeling.

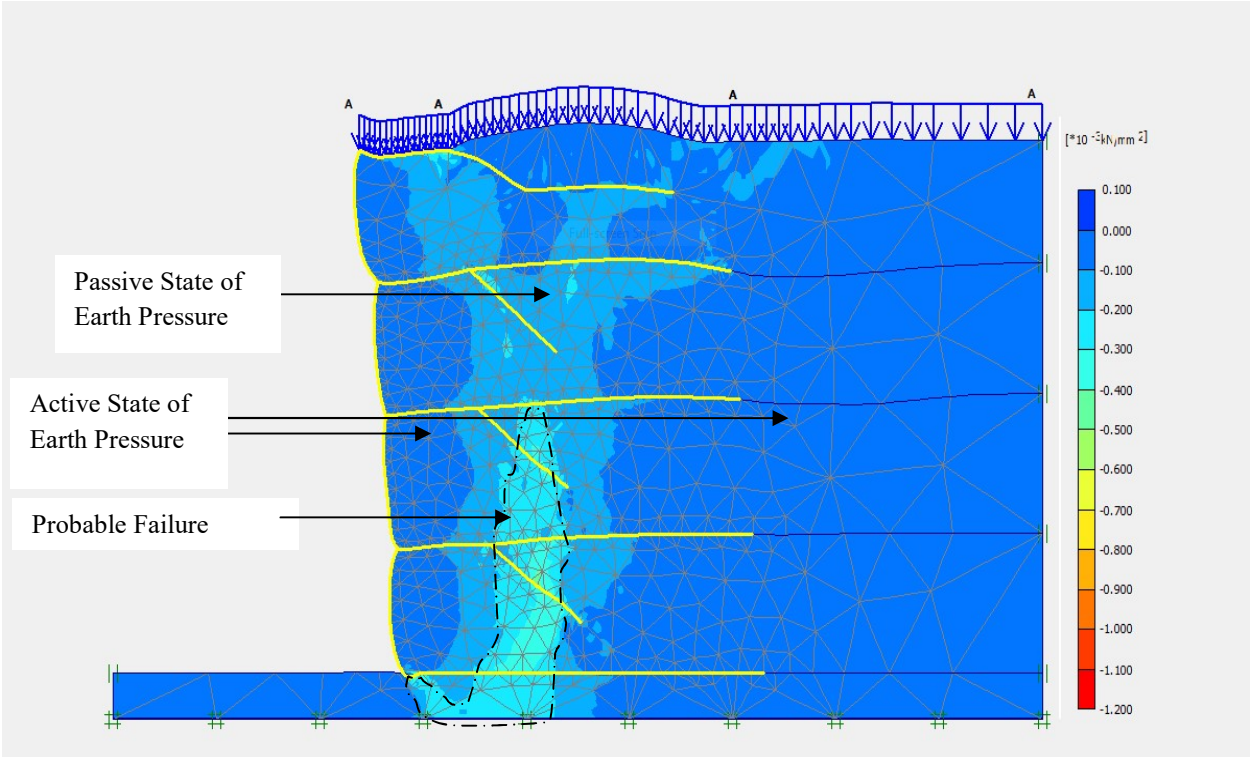


Figure 5.9 Mean Stresses

### 5.4.3 Failure of MSE Wall

Plastic points are defined as the stress points in a plastic state. The plastic stress points are represented by red open squares. The tension cut-off points are represented by black solid fill squares. Both of them, at the final stage have been depicted in Figure 5.10. Plastic point indicates that the stresses lie on the surface of the Coulomb failure envelope. From Figure 5.10, it can be observed that many plastic points occur near the face of the wall. This coupled with many cut-off points near the toe of the wall, helps to predict that the wall will undergo an overturning failure.

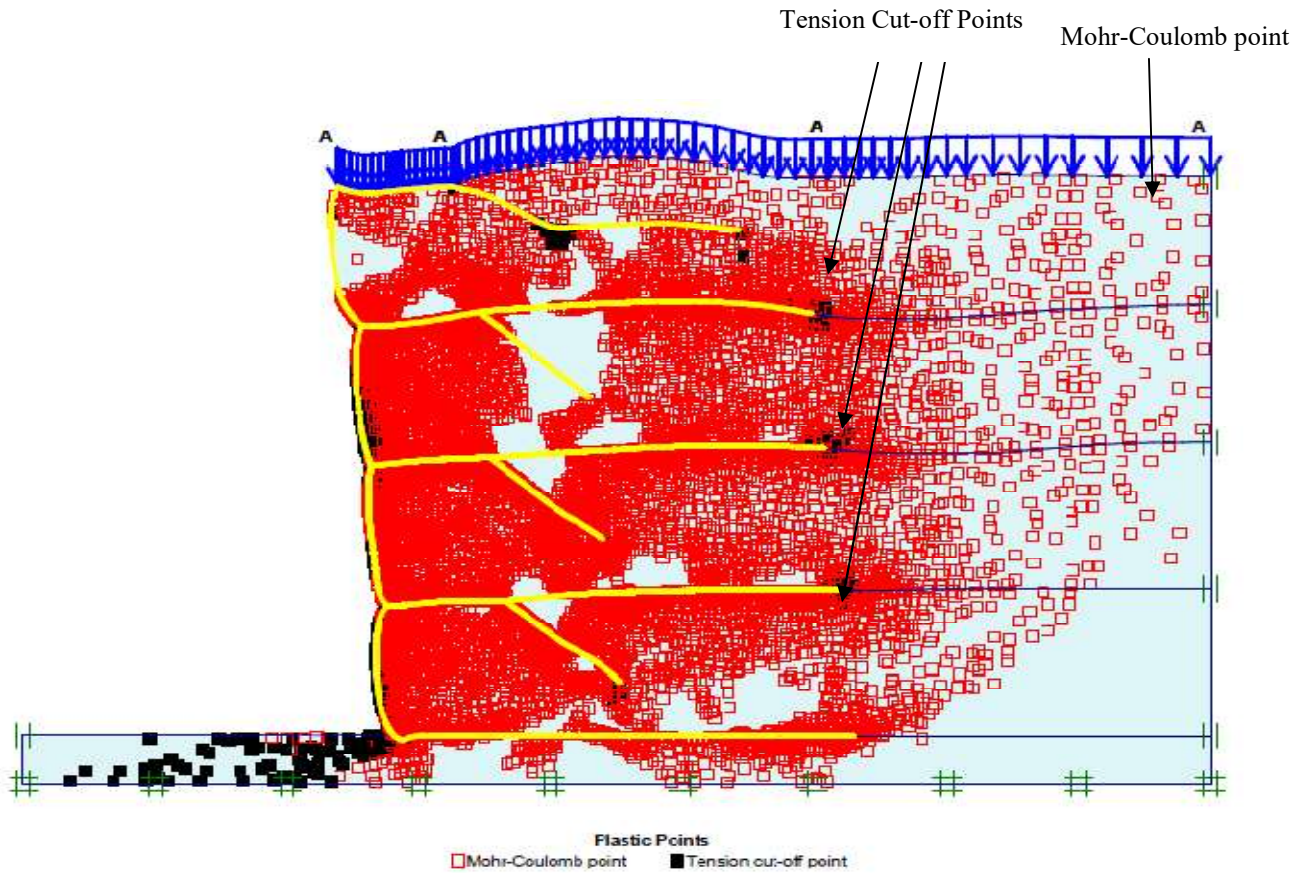


Figure 5.10 Plastic Points

## 5.5 Validation of Experimental Testing by Numerical Modeling

The deformation pattern obtained in both, experimental and numerical analysis complement each other. The results representing the same have been shown below in Figure 5.11 (a) and Figure 5.11 (b). The top most layer in both, experimental and numerical analysis is deemed to have undergone the maximum horizontal displacement which is clearly shown in the mentioned figures. Results from both the analysis, indicate that the wall has a tendency to undergo overturning failure. The validation of physical deformation by both the analysis justifies our study.

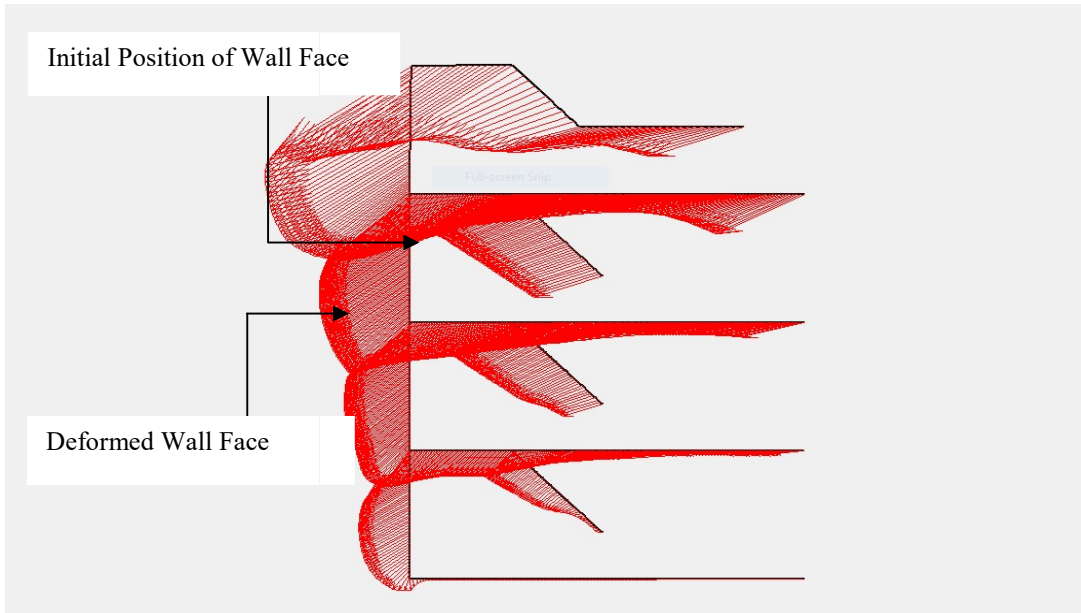


Figure 5.11(a) Deformed Wall from Numerical Modeling

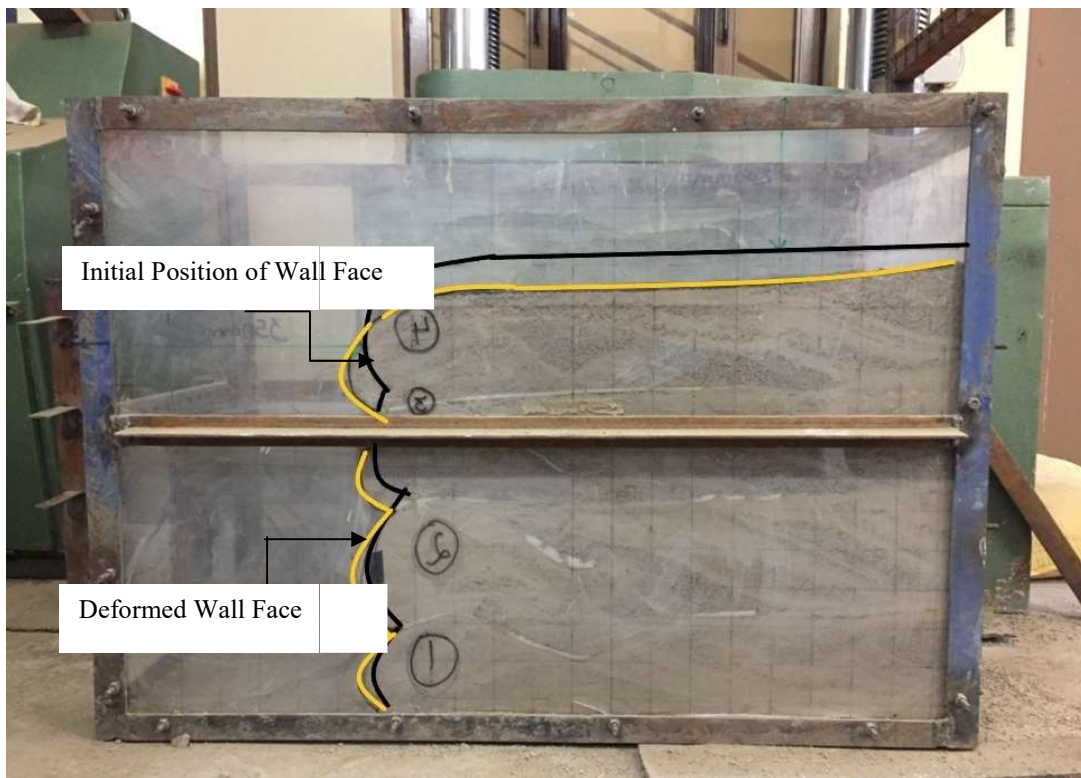


Figure 5.11(b) Deformed Wall from Model Testing

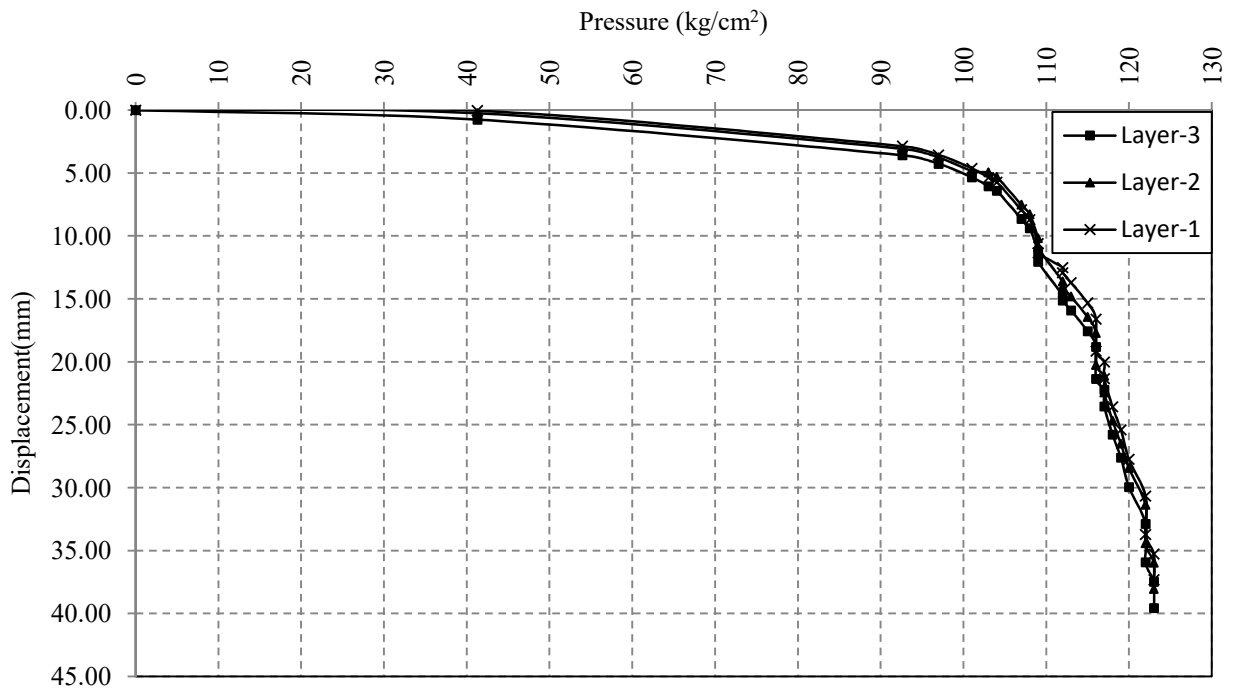


Figure 5.12 (a) Horizontal Displacement from Numerical Modeling

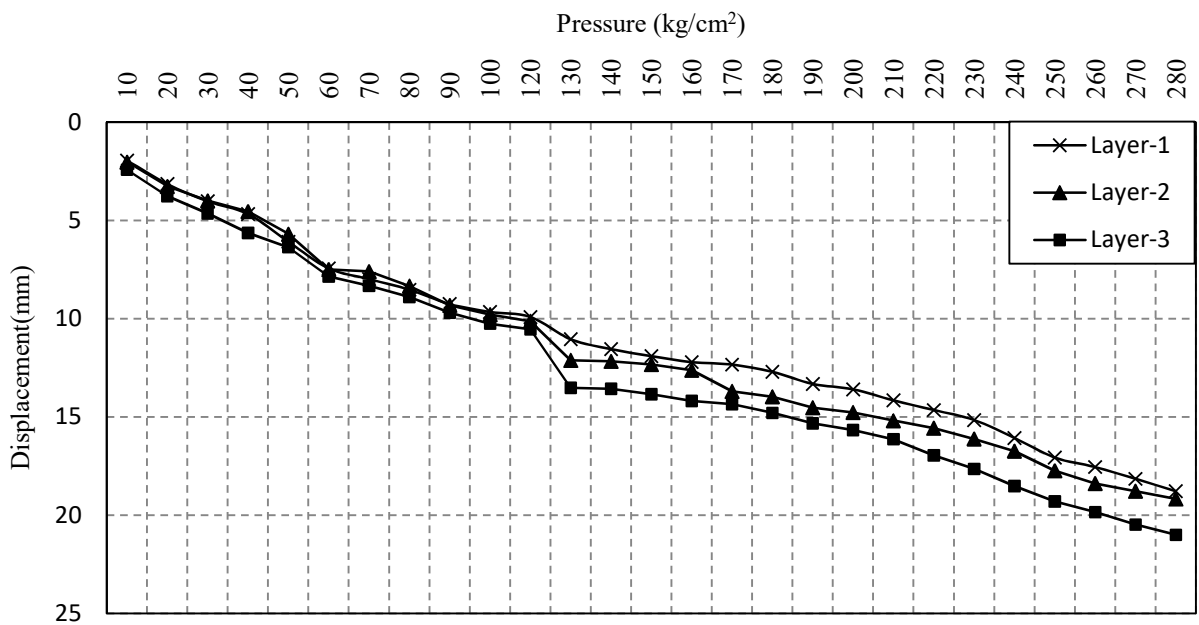


Figure 5.12 (b) Horizontal Displacement from Model Testing

From the above obtained plots, Figure 5.12 (a) and 5.12 (b) of horizontal displacement from both the analysis, numerical and experimental namely, it can be observed that the model under experimental testing undergoes a larger amount of displacement for the same load when compared to numerical modeling. This is due to the fact that in experimental modeling the soil undergoes compression and rearrangement of particles, whereas the numerical analysis develops around the values of unit weight provided to it and the simulation operates in an ideal condition. After a value of  $100 \text{ kg/cm}^2$  of the applied pressure both the graphs exhibit the same nature, that is, a greater increase in displacement with a corresponding smaller increment in applied pressure.

The pattern continues in numerical modeling, that is, for a small increment in the pressure applied, a larger value of displacement is obtained. But the same pattern, from here on, does not replicate in the experimental modeling. The reasons which can be attributed to this mismatch are the ideal condition simulations in the case of numerical modeling. In experimental modeling, the soil mass is confined due to the presence of perspex sheet which reduces the displacement of the expanding soil. This reason coupled with warping of the surcharge plate does not allow complete transfer of load from the hydraulic jack to the soil mass, as some portion of the pressure is absorbed by these two elements. The maximum horizontal displacement obtained in experimental modeling is 21mm and in numerical modeling is 39.55 mm, and the reasons for this difference have been discussed above.

From the obtained plots shown in Figure 5.13 (a) and 5.13 (b) of vertical displacement from both the analysis, it can be observed that both the plots complement their corresponding horizontal displacement graphs. One difference can be observed between the vertical displacement plots of experimental and numerical testing. The difference between the maximum horizontal and maximum vertical is lower in numerical modeling as compared to experimental modeling. This can be due to the fact that the Perspex sheet is not able to act as a rigid boundary and undergoes warping. This results in a decrease in horizontal displacement due to the lateral expulsion of the soil, which is the reason we obtain a greater difference in maximum horizontal and vertical displacement in the case of experimental testing.

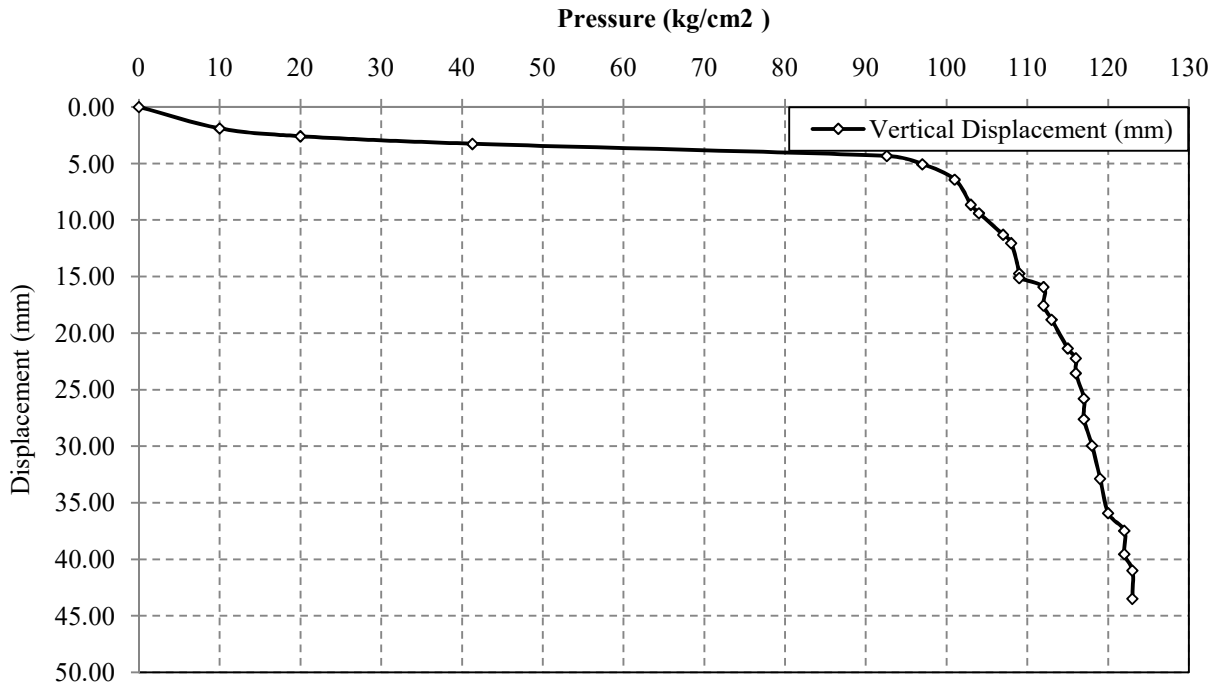


Figure 5.13 (a) Vertical Displacement from Numerical Modeling

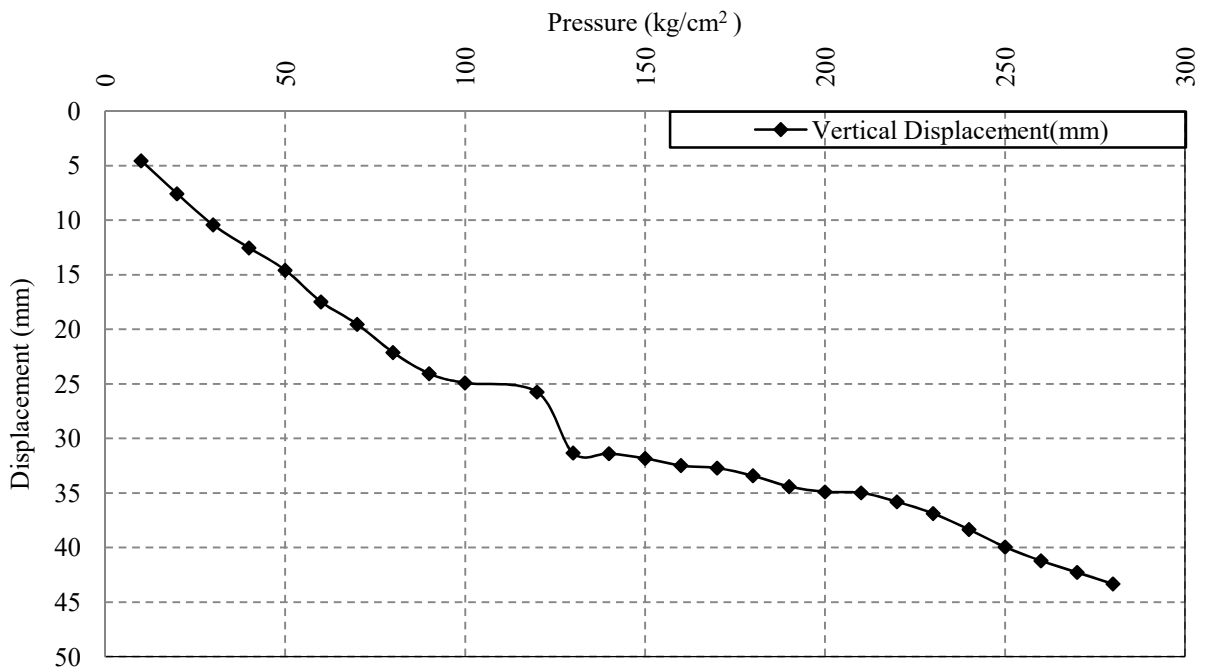


Figure 5.13 (b) Vertical Displacement from Model Testing

# CHAPTER 6

## CONCLUSION

---

### 6.1 General

We performed the experimental and numerical testing of the MSE wall. It can be concluded that the technique of soil reinforcement has evolved and contributed to the infrastructure in terms of speed, ease of construction, economy and aesthetics.

### 6.2 Conclusions

From the study undertaken, we can now conclude that the technique of soil reinforcement utilizing geosynthetics is a revolution. Following are the conclusion of our study.

- This technique is economic and requires very less skilled workers when compared to the conventional soil retaining structures.
- In the present study, the load-displacement characteristics were studied under experimental modeling. After studying the results, it can be concluded that the wall responded in an effective manner and showcased a potential for replacing the conventional soil retaining structures.
- Methodology adopted in the development of numerical model to stimulate the physical model tests is explained along with the validation of numerical model with the physical model.
- Results from the test on physical and numerical models of geotextile-reinforced wrap-around soil retaining walls are presented and compared.
- The numerical model developed is reasonably good in simulating the load displacement response of wrap faced wall model.
- The study concluded that amongst all the parameters, dilation and friction angle of the soil mass and the stiffness of the reinforcing geotextile are the most affecting parameters.

### 6.3 Scope for Future Work

After having concluded the study and validating the experimental analysis with the help of numerical modeling results, this chapter goes on further to discuss at length the scope for future work in the field of soil reinforcement, and more particularly, MSE wall retaining structure.

For our study we have utilized a constant  $L_{\text{rein}}/H$  ratio, but as stated in many literatures, the  $L_{\text{rein}}/H$  ratio can be varied to study the resultant behavior of the soil reinforced structure. Therefore a study of change in  $L/H$  ratio deems to a future prospect in this field. Our study mainly focuses on the static loading of the structure, but we leave open a Pandora box which deals with dynamic loading of the structure. If under dynamic loading, the structure responds efficiently, then it can be used as an alternative to traditional retaining structures in zones of high seismic activity.

The present study has focused on the fabrication and analysis of the wrap-faced MSE wall, whereas there exist a huge range of wall facings which can be incorporated in the structure. What do wall facings do the structure, remains a matter out of scope of this study yet they add an aesthetic view to the structure.

The next set of future prospects for the study includes varying the backfill used or using backfill with poor drainage capability. The retained and reinforced backfill soil can be different and the result of such a combination can be obtained and discussed. Despite being a concept so old, the economic soil reinforcing techniques have not been able to take over the traditional ones, and hence this calls for more research in this field with various varying parameters and suitability to all conditions.

## REFERENCES

---

1. San, K. C., Leshchinsky, D. and Matsui, T. (1994) - "Geosynthetic Reinforced Slopes: Limit Equilibrium & Finite Element Analysis." *Soils and Foundations*, Japanese Society of Soil Mechanics and Foundation Engineering, 34(2),79-85
2. Scarborough, J.A. (2004). "A Tale of Two Walls: Case Histories of Failed MSE Walls." *Slopes and Retaining Structures under Seismic and Static Conditions*, Auburn University
3. Koerner, R.M. (2005). "Designing for Soil Reinforcement." *Designing with Geosynthetics*, University of Michigan, 198-199
4. Berg, R.R. et al. (2009). "Design and Construction of Mechanically Stabilized Earth Walls and Reinforced Soil Slopes – Volume I." U.S. Department of Transportation Federal Highway Administration, Washington, 42-82
5. Hardianto, F.S. et al. (2010). "A Review of Seismic LRFD (Load-and-resistance Factor Design) Method For MSE (Mechanically Stabilized Earth) Walls." *Fifth International Conference on Recent Advances in Geotechnical Earthquake Engineering and Soil Dynamics*, San Diego, California, 1-9
6. Agrawal, B.J. (2011). "Geotextile: It's application to civil engineering - Overview." *National Conference on Recent Trends in Engineering & Technology*, V.V.Nagar, Gujarat, 1-6
7. Krishna, A.M. and Latha, G.M. (2012). "Modeling of dynamic response of wrap faced reinforced soil retaining wall." *International Journal of Geomechanics*, ASCE, 12(4), 439-450
8. Babu, G.L.S (2012). "Reinforced Soil Retaining Walls - Design and Construction." <http://nptel.ac.in/courses/105108075/module8/Lecture31.pdf> (October 4,2012)

9. Skejic, A. et al. (2013). "Observation and Numerical Modeling of Test MSEW with Inextensible Inclusions and Coarse Crushed Stone Backfill." *Electronic Journal of Geotechnical Engineering*, 18, 7-16
10. Kibria, G. et al. (2014). "Influence of Soil Reinforcement on Horizontal Displacement of MSE Wall." *International Journal of Geomechanics*, ASCE, 14(1), 5-8
11. Mandal, J.N. (2014). "Geosynthetics Engineering: In Theory & Practice." <http://nptel.ac.in/courses/105101143/downloads/Lecture%2026.pdf>(April 15, 2014)
12. Balakrishnan, S. and Viswanadham, B.V.S. (2015). "Performance evaluation of geogrid reinforced soil walls with marginal backfills through centrifuge model tests." *Elsevier Ltd*, 1-14
13. Singh, H. and Akhtar, S. (2015). "A Review on Economic Analysis of Reinforced Earth Wall with Different Types of Reinforcing Materials." *International Journal of Latest Technology in Engineering, Management & Applied Science (IJLTEMAS)*, 4 (12), 68-74
14. Infante, D.J.U et al. (2016). "Shear Strength Behavior of Different Geosynthetic Reinforced Soil Structure from Direct Shear Test." *International Journal of Geosynthetics and Ground Engineering* ,Springer International Publishing Switzerland, 1-16

## ANNEXURE A

Table 1 Readings of horizontal displacement with pressure applied

Pressure (kg/cm <sup>2</sup> )	Layer-1 (mm)	Layer-2 (mm)	Layer-3 (mm)
10	1.96	2.43	2.03
20	3.15	3.77	3.27
30	4.03	4.65	4
40	4.68	5.64	4.55
50	6.09	6.37	5.7
60	7.44	7.86	7.5
70	7.99	8.33	7.6
80	8.53	8.9	8.34
90	9.26	9.7	9.32
100	9.66	10.26	9.79
120	9.92	10.55	10.13
130	11.05	13.52	12.12
140	11.55	13.57	12.17
150	11.91	13.85	12.33
160	12.21	14.19	12.62
170	12.34	14.35	13.7
180	12.71	14.8	13.97
190	13.32	15.33	14.53
200	13.6	15.67	14.77
210	14.16	16.14	15.19
220	14.65	16.96	15.57
230	15.16	17.65	16.12
240	16.07	18.52	16.74
250	17.07	19.3	17.74
260	17.55	19.85	18.39
270	18.15	20.48	18.78
280	18.78	21	19.17

## ANNEXURE B

Table 2 Readings of vertical displacement with pressure applied

Pressure (kg/cm <sup>2</sup> )	Vertical Displacement (mm)
10	4.56
20	7.59
30	10.44
40	12.55
50	14.59
60	17.49
70	19.55
80	22.13
90	24.07
100	24.93
120	25.76
130	31.35
140	31.41
150	31.85
160	32.5
170	32.73
180	33.44
190	34.42
200	34.91
210	35
220	35.82
230	36.89
240	38.36
250	39.96
260	41.22
270	42.3
280	43.35

## ANNEXURE C

Table 3 Readings of strains developed with pressure applied

Pressure (kg/cm <sup>2</sup> )	R <sub>L1</sub>	R <sub>L2</sub>	R <sub>L3</sub>	Strain-1	Strain-2	Strain-3
10	220	225	221	0.203714418	0.20770037	0.203813526
20	221	226	222	0.203964384	0.207950491	0.204064425
30	221	226	222	0.203964384	0.207950491	0.204064425
40	222	227	223	0.204214168	0.208200428	0.204315139
50	222	227	223	0.204214168	0.208200428	0.204315139
60	223	228	224	0.204463769	0.208450182	0.20456567
70	223	228	224	0.204463769	0.208450182	0.20456567
80	224	228	225	0.204713187	0.208450182	0.204816018
90	225	228	226	0.204962424	0.208450182	0.205066182
100	225	228	227	0.204962424	0.208450182	0.205316164
110	226	229	228	0.205211479	0.208699753	0.205565962
120	226	230	229	0.205211479	0.208949141	0.205815578
130	230	234	235	0.206205886	0.209944872	0.207309449
140	231	234	236	0.206454035	0.209944872	0.207557792
150	232	235	237	0.206702004	0.21019335	0.207805954
160	233	235	238	0.206949792	0.21019335	0.208053935
170	234	235	238	0.2071974	0.21019335	0.208053935
180	235	236	239	0.207444829	0.210441646	0.208301736
190	236	237	241	0.207692077	0.210689762	0.208796795
200	237	238	243	0.207939146	0.210937696	0.209291135
210	238	242	245	0.208186035	0.211927625	0.209784756
220	238	245	247	0.208186035	0.212668181	0.21027766
230	239	246	248	0.208432745	0.212914674	0.210523844
240	239	248	250	0.208432745	0.213407121	0.211015675
250	240	249	252	0.208679276	0.213653076	0.211506793
260	242	249	254	0.209171802	0.213653076	0.2119972
270	244	250	256	0.209663615	0.213898853	0.212486896
280	245	250	258	0.209909254	0.213898853	0.212975884

# JAYPEE UNIVERSITY OF INFORMATION TECHNOLOGY, WAKNAGHAT LEARNING RESOURCE CENTER

## PLAGIARISM VERIFICATION REPORT

Date:

Type of Document (Tick):  Thesis  M.Tech Dissertation/ Report  B.Tech Project Report  Paper

Name: Manik Uppal, Hannaan Malik Department: Civil Engineering

Enrolment No. 141690, 141692 Registration No. \_\_\_\_\_

Phone No. 7006322324, 9805047873 Email ID. malik.hannaan@gmail.com

Name of the Supervisor: Dr. Saurabh Rawat

Title of the Thesis/Dissertation/Project Report/Paper (In Capital letters): \_\_\_\_\_

TESTING AND NUMERICAL MODELING OF MECHANICALLY  
STABILIZED EARTH WALL REINFORCED WITH GEOTEXTILE.

Kindly allow me to avail Turnitin software report for the document mentioned above.

Manik Hannaan  
(Signature)

### FOR ACCOUNTS DEPARTMENT:

Amount deposited: Rs. 300/- Dated: 12.5.18 Receipt No. BRN1805/339  
(Enclosed payment slip)

[Signature]  
(Account Officer)

### FOR LRC USE:

The above document was scanned for plagiarism check. The outcome of the same is reported below:

Copy Received on	Report delivered on	Similarity Index in %	Submission Details	
			Word Counts	Character Counts
<u>14/05/2018</u>	<u>15/05/2018</u>	<u>19%</u>	<u>14,283</u>	<u>72,396</u>
			<u>72</u>	<u>4.97M</u>
			Page counts	
			File Size	

Checked by [Signature]  
Name & Signature

[Signature]  
Librarian

LIBRARIAN  
LEARNING RESOURCE CENTER  
Jaypee University of Information Technology  
Waknaghat, Distt, Solan (Himachal Pradesh)  
Pin Code: 173234